

APPENDIX A

**A General Model of Coal Devolatilization
(revised - Accepted for Publication in Energy & Fuel)**

April, 1988

A GENERAL MODEL OF COAL DEVOLATILIZATION

P.R. Solomon⁺, D.G. Hamblen, R.M. Carangelo, M.A. Serio and G.V. Deshpande

Advanced Fuel Research, Inc., 87 Church St., East Hartford, CT 06108 USA

ABSTRACT

A general model for coal devolatilization which combines a functional group model for gas evolution and a statistical model for tar formation has been presented. The tar formation model includes depolymerization, crosslinking, external transport and internal transport. The crosslinking is related to the evolutions of CO₂ and CH₄, with one crosslink formed per molecule evolved. The model predictions compare favorably with a variety of data for the devolatilization of Pittsburgh Seam coal and North Dakota (Beulah) lignite, including volatile yields, extract yields, crosslink densities and tar molecular weight distributions. The variations with pressure, devolatilization temperature, rank and heating rate were accurately predicted. Comparison of the model with several sets of data employing alternative assumptions on transport suggests assuming that the particle is well mixed (i.e. the surface concentration of tar molecules is the same as the bulk) overpredicts the transport rate. For 50 μm particles, assuming that the internal transport limitation dominates (i.e. neglecting the external transport) provides a good fit to the data. The rank dependence of tar formation, extract yields, crosslinking, and viscosity appears to be explained by the rank dependence of CO₂ yields and its associated crosslinking. High CO₂ yields in low rank coals produces rapid crosslinking at low temperatures and hence thermosetting behavior, low tar yields, low extract yields, loss of solvent swelling properties and high viscosities. The relative importance of crosslinking compared to bond breaking is, however, sensitive to heating rate and this effect is predicted by the model. Areas for improving the model include: 1) refinement of the internal and external transport assumptions; 2) accounting for hydroaromatic structures and bridge structures besides ethylene; 3) including polymethylene "guest" molecules.

A GENERAL MODEL OF COAL DEVOLATILIZATION

P.R. Solomon⁺, D.G. Hamblen, R.M. Carangelo, M.A. Serio and G.V. Deshpande

Advanced Fuel Research, Inc., 87 Church St., East Hartford, CT 06108 USA

INTRODUCTION

Coal devolatilization is a process in which coal is transformed at elevated temperatures to produce gases, tar* and char. The combined chemical and physical processes in devolatilization have been reviewed by a number of investigators (1-6). Gas formation can often be related to the thermal decomposition of specific functional groups in the coal and can be predicted with reasonable accuracy by models employing first order reactions with ultimate yields (5-15). On the other hand, tar and char formation are more complicated and success in mechanistic modeling of tar formation has been more limited.

Predicting tar formation is, however, important for several reasons. Tar is a major volatile product (up to 40% of the DAF coal weight for some bituminous coals). Tar yields vary substantially depending on reactor conditions (pressure, heating rate, final temperature, bed geometry, particle size, etc.). In combustion or gasification, tar is often the volatile product of highest initial yield and thus controls ignition and flame stability. It is a precursor to soot which is

*Tar is defined as the room temperature condensibles formed during coal devolatilization.

⁺ To whom correspondence is to be sent.

important to radiative heat transfer. The process of tar formation is linked to the char viscosity (16-19) and the subsequent physical and chemical structure of the char, and so is important to char swelling and reactivity. Also, because tar molecules are sometimes minimally disturbed coal molecular fragments, primary tars provide important clues to the structure of the parent coal (5,6,20).

It is generally agreed that the tar formation includes the following steps: 1) depolymerization by rupture of weaker bridges in the coal macromolecule to release smaller fragments which make up the "metaplast" (3,5,7,16,21-33); 2) repolymerization (crosslinking) of metaplast molecules (3,5,7,16,21-33); 3) transport of lighter molecules away from the surface of the coal particles by combined vaporization and gas phase diffusion (23,32); 4) internal transport of lighter molecules to the surface of the coal particles by convection and diffusion in the pores of non-softening coals (24,27,34,35) and liquid phase or bubble transport in softening coals (17,36-38). Char is formed from the unreleased or recondensed fragments. Varying amounts of loosely bound "guest" molecules, usually associated with the extractable material, are also released in devolatilization.

The complexity of proposed devolatilization models varies substantially. They can be divided into four categories. The simplest are the "Weight Loss Models" employing a single rate (6,22,39-42), two rates (39,43), multiple parallel rates or distributed rates (9,22). These models do not account for the variations in tar yield with reaction conditions and a number of "Tar Formation Models" incorporating retrogressive char forming reactions and mass transport have been proposed which account for such variations (16,21-33,37,44-49). A recent innovation has been the description of the decomposition and repolymerization of the macromolecular network using statistical methods (28,29,44-46,50,51).

Most of the above models do not consider the evolution of gas species, which have been treated in a number of "Species Evolution/Functional Group Models" as parallel first order reactions (5-13). More complicated "Comprehensive Chemical Models" also describe the composition of the char and tar (3,5,6,11-13,33,48,49, 51).

The level of detail required in a model depends on its application. In modeling combustion and gasification the simple "Weight Loss Models" have often been employed. However, to predict the variations in yield with reactor conditions, the more complicated "Tar Formation Models" must be used. A case can also be made for employing "Species Evolution/Functional Group Models" or "Comprehensive Chemical Models". For example, in predicting the energy released from combustion of the volatiles it is important to know that for low rank coals a high percentage of the volatiles may be non-combustible H_2O and CO_2 . For a North Dakota lignite, the total of these two components can be as high as 35% of the rapidly released volatiles which are important for ignition (6). In addition, the swelling, particle agglomeration properties, char reactivity, and char fragmentation are functions of the char composition. Soot formation (which can dominate radiative energy transport) is controlled by the tar amount.

In modeling liquefaction and mild gasification, knowledge of the chemical makeup and molecular weight distribution of the soluble and volatile products is essential, requiring the more complete "Comprehensive Chemical Models".

This paper presents a "comprehensive chemical model" for coal devolatilization which considers the evolution of gas, tar, char and gaseous molecules. The model is general in its applicability to bituminous coals, subbituminous coals and lignites (employing rank independent kinetic parameters), in its application to reactors of

widely differing heating rates (0.05°C/sec to 20,000°C/sec) and in its ability to predict the variations in tar yield with reactor conditions.

Two previously developed models, a Functional Group (FG) model (5,6,11-13) (a "Species Evolution/Functional Group Model") and a Devolatilization-Vaporization-Crosslinking (DVC) model (30,31,44-47) (a "Tar Formation Model") have been combined as subroutines of what is now called the "FG-DVC" model (33,50,51). The DVC subroutine is employed to determine the yield of tar and the molecular weight distribution of the tar and char. The FG subroutine is used to describe the gas evolution, and the elemental and functional group compositions of the tar and char. Crosslinking in the DVC subroutine is computed by assuming that this event is correlated with CO₂ and CH₄ evolutions predicted in the FG subroutine. The dependence of the yield of rapidly released CO₂ (which is related to coal rank or weathering) is the factor which controls the thermosetting or thermoplastic behavior of coals.

The combined FG-DVC model was described in two previous publications (50,51) and comparisons were made to a limited set of data. In this paper, a description of internal transport has been added to the model. The model equations are presented and comparisons are made to a wider set of data. The paper also includes a discussion of the assumptions, approximations and exceptions to the model and a sensitivity analysis for the parameters of the DVC subroutine. The model describes the processes of:

- 1) Depolymerization and Hydrogen Consumption
- 2) Crosslinking
- 3) External Transport
- 4) Internal Transport

- 5) Gas Formation for all principal species
- 6) Tar Composition
- 7) Char Composition

The work presented here is limited to dilute phase reactions of small coal particles where internal temperature gradients can be neglected. Secondary gas phase reactions have been discussed elsewhere (6) and reactions of pyrolysis products with a char bed and large particle effects have not yet been included. Only reactions involving C, H, and O are discussed here.

A number of coal composition parameters and reactor parameters (pressure, particle time-temperature history) are required to predict the pyrolysis behavior. A substantial reduction in the number of parameters which must be measured for each coal is made by the use of rank independent kinetic rates. These parameters have already been determined using a wide variety of coals and reactors. This simplification is a good first approximation to describe the kinetics of individual evolved species and the functional group decompositions (5,6,49,52-55). The properties predicted as a function of time, include: **TAR** - molecular weight distribution, elemental and functional group composition, yield; **CHAR** - molecular weight distribution, elemental and functional group composition, yield, crosslink density, extract yield; **GAS** - yields of individual light gas species. Results are presented for a Pittsburgh Seam bituminous coal and a North Dakota lignite.

EXPERIMENTAL

Coals Examined. The two coals described in this paper are a Pittsburgh Seam bituminous coal and a North Dakota (Beulah, Zap) lignite. Samples of the Pittsburgh Seam coal were obtained from the Pittsburgh Energy Technology Center and

the Argonne National Laboratory premium coal sample collection. Samples of the North Dakota (Beulah, Zap) lignite were obtained from the University of North Dakota Energy Research Center and the Argonne National Laboratory premium coal sample collection. Data on the premium samples are presented in Ref. 56 and on the other two samples in Ref. 6. The FG-DVC model was also compared to data on Pittsburgh coal samples from Refs. 7, 16 and 22, and characterizations of these samples are presented therein.

Coal Characterization. The crosslink density was estimated using the volumetric swelling technique developed by Larsen and co-workers (57-59). Pyridine extract yields were obtained using a Soxhlet apparatus. Molecular weight distributions of tars were obtained at SRI International using the Field Ionization Mass Spectrometry (FIMS) apparatus described by St. John et al. (50). Tar samples were collected from the pyrolysis apparatus and vaporized from a heated probe into the FIMS apparatus. In addition, coal samples were pyrolyzed directly in the FIMS apparatus.

Apparatus. Pyrolysis experiments were performed in several apparatuses which have been described previously including: a heated grid pyrolyzer (5,12), a heated tube reactor (6,13), and a thermogravimetric analyzer with analysis of evolved products by Fourier Transform Infrared (FT-IR) Spectroscopy (TG-FTIR) (6,61).

GENERAL MODEL

Any general model of a process as complicated as coal devolatilization must of course be a gross approximation. However, there are many general trends which have been observed in devolatilization. The trick in developing a model is to pick a set of first approximations which best match the majority of these trends. There

will of course be exceptions to the trends. These exceptions can be treated as perturbations to the first order approximation. Differences in models occur because of the subjective choice of what is a general trend and what is an exception. The following discussion presents the authors' view of the general trends and the exceptions.

The General Trends in Devolatilization.

The general model of coal pyrolysis is based on a number of observations which have been previously made concerning coal pyrolysis. These are: i) pyrolysis species kinetics are insensitive to rank (5,6,11-13,52-55); ii) species amounts vary with coal rank and can be correlated with the coal's functional group compositions (5,6,14,15,48,49,52). The evolution of each species can be correlated with the change in the corresponding functional group composition in the char (5,6,52); iii) the primary tar composition is similar (except for a higher concentration of methyl groups) to that of the parent coal for bituminous coals and rapidly heated low rank coal (5,20,45,62-64); iv) tar yields are controlled by the amount of donatable hydrogen and how efficiently it is used (5,6,20,46); and v) crosslinking correlates with CO₂ and CH₄ evolution (51,52).

The general outline of devolatilization based on these observations was presented by Solomon and Hamblen (5) and Serio et al. (6). Fig. 1 from Ref. 6 presents a hypothetical picture of the coal's or char's organic structure at successive stages of devolatilization. The figure represents: a) the raw coal, b) the formation of tar and light hydrocarbons during primary pyrolysis, and c) char condensation and crosslinking during secondary pyrolysis. The hypothetical structure in Fig. 1a represents the chemical and functional group compositions for a Pittsburgh Seam bituminous coal as discussed by Solomon (20). It consists of

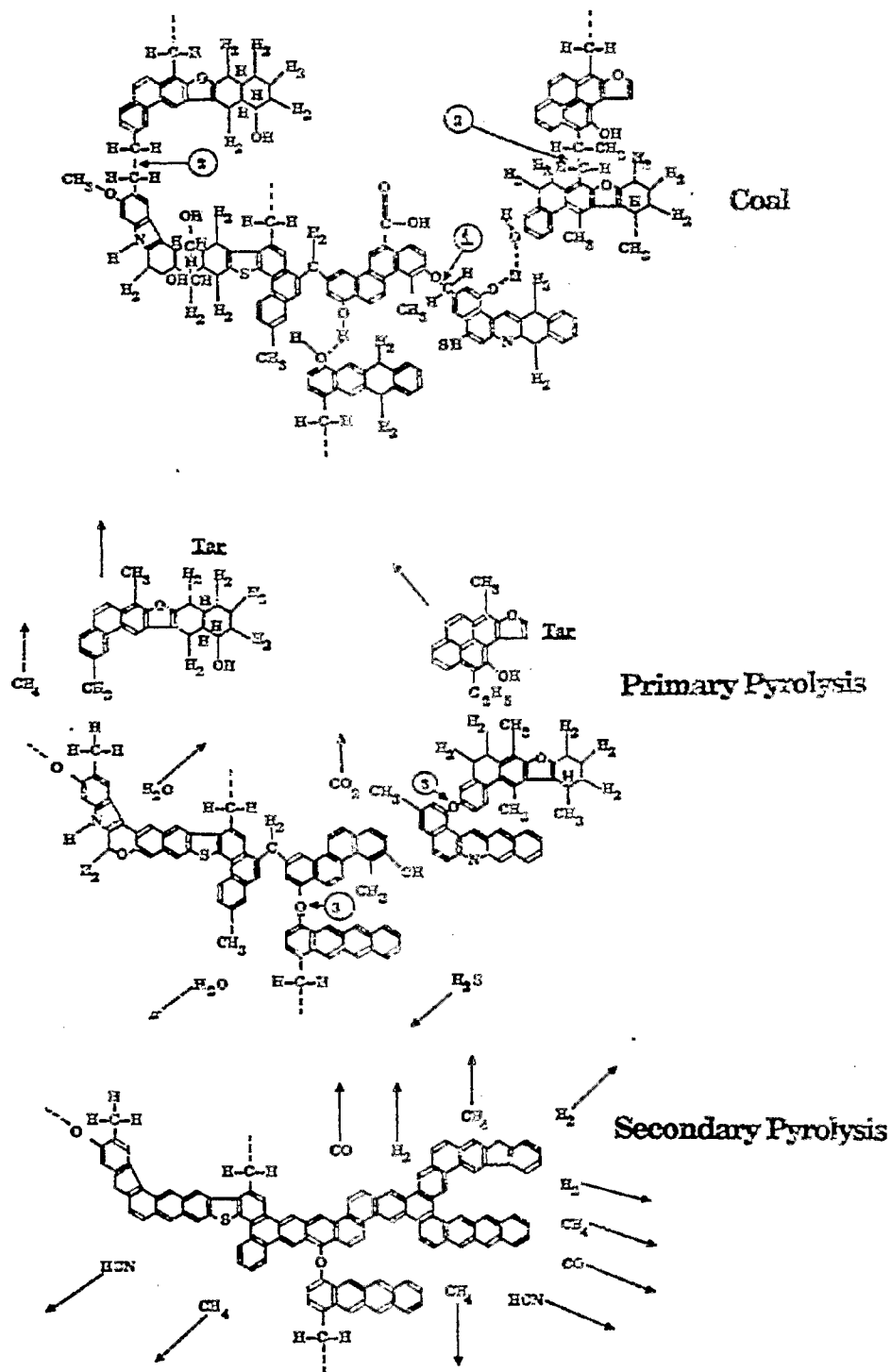


Figure 1. Hypothetical Coal Molecule During Stages of Pyrolysis.
 (Reprinted from Reference 6 with permission).

aromatic and hydroaromatic clusters linked by aliphatic bridges. During pyrolysis, the weakest bridges, labeled 1 and 2 in Fig. 1a, can break producing molecular fragments (depolymerization). The fragments abstract hydrogen from the hydroaromatics or aliphatics, thus increasing the aromatic hydrogen concentration. These fragments will be released as tar if they are small enough to vaporize under typical pyrolysis conditions and do not undergo retrograde reactions before escaping from the particle. The two lightest fragments are labeled tar. The other two fragments are shown to have repolymerized, producing a molecule which is too large to vaporize.

The other events during primary pyrolysis are the decomposition of functional groups to release CO_2 , light aliphatic gases and some CH_4 and H_2O . The release of CH_4 , CO_2 , and H_2O may produce crosslinking, CH_4 by a substitution reaction in which the attachment of a larger molecule releases the methyl group, CO_2 by condensation after a radical is formed on the ring when a carboxyl is removed and H_2O by the condensation of two OH groups to produce an ether link (labeled 3 in Fig. 1b). The crosslinking is important to determine the release of tar and the visco-elastic properties of the char.

The end of primary pyrolysis occurs when the donatable hydrogens from hydroaromatic or aliphatic portion of the coal are depleted. During secondary pyrolysis (Fig. 1c) there is additional methane evolution (from methyl groups), HCN from ring nitrogen compounds, CO from ether links, and H_2 from ring condensation. These general concepts are incorporated into the combined FG-DVC model.

The Exceptions to the General Trends.

a. **Polymethylene.** The major exception to the trends described above is the

presence of varying amounts (typically 0 to 9%, but in some cases as high as 18%) of long chain aliphatics (polymethylenes). These have recently been reported in pyrolysis products by Nelson (65), by Calkins and co-workers (66-69), and references quoted therein. The chains appear alone and attached to aromatic nuclei (65). During devolatilization, the smaller molecules may be released without bond breaking and the heavier molecules with bond breaking to contribute to the tar. The presence of these polymethylenes makes the tar more aliphatic than the parent coal. Further cracking of this material under more severe devolatilization conditions produces ethylene, propylene and butadiene from which the concentration of polymethylenes may be determined (68). Presently, the polymethylenes are included in the FG model as part of the aliphatic functional group pool, which is assumed to decompose to produce gas products, not tar. If the amount of heavy polymethylenes is determined, these can be computed as a separate functional group pool with an appropriate release rate and added to the tar. The modeling of polymethylene evolution will be the subject of a subsequent publication.

b. Tar/Coal Similarities. The general model assumed, as a first approximation, that tar is derived from material of the same average composition as that of the parent coal. The model predicts that the tar is richer than the parent coal in methyl groups (due to hydrogen stabilization) and poorer in the rapidly removed functional groups. Evidence for this assumption is the similarities in elemental composition, infrared spectra and NMR spectra (5,20,45,62-64) between the primary tar and parent coal observed for bituminous coals. It was, however, noted (5,45,70) that the infrared spectrum for a lignite tar was significantly different from that of the parent coal. The tar is much richer in aliphatic groups and poorer in oxygen functional groups. Freihaut et al. have recently reported a

systematic increase in the tar hydrogen concentration with decreasing rank which suggests a similar trend (71).

There are at least two reasons for this variation with rank. One reason is the influence of the polymethylene groups. As noted by Calkins (68), the concentration of polymethylenes increases with decreasing rank (~4% for high volatile bituminous coals compared to ~8% for lignites). In addition, the tar yield decreases with decreasing rank, (~6% for the North Dakota lignite compared to 30% for the Pittsburgh Seam bituminous coal). The relative contribution of the polymethylenes to the tar is therefore increased with decreasing rank. This will lead to a higher aliphatic content and lower oxygen content for the low rank coal tar. This effect can be treated in the FG-DVC model by the addition of polymethylenes to the tar as discussed above.

A second reason for differences in structure between the tar and parent coal is that the extensive crosslinking in low rank coals is related to the carboxyl group concentration, which increases with decreasing rank. This crosslinking will thus selectively repolymerize the fragments rich in oxygen, while those poorer in oxygen are more likely to be released as tar. This effect has not as yet been included in the model.

It is interesting to note an exception to the above observations. At very high heating rates, the North Dakota (Beulah, Zap) lignite is observed to melt and swell and produce a higher yield of tar which resembles the parent coal (13,30,31). The high heating rate appears to reduce the effect of crosslinking, leading to higher oxygen concentrations in the tar and to increased yields. Both effects enhance the resemblance to the parent coal.

c. **Variations of Kinetic Rates with Rank.** While the model assumes rank independent kinetic rates, there is a systematic variation of rate with rank. As reported by Solomon and Hamblen (52), the variation between a lignite and bituminous coal results in a 50-75°C difference in the peak evolution temperature for most species (at a heating rate of 30 K/min). Systematic rank variations in the rate constants can be added to the model if increased accuracy is desired.

d. **Macerals.** Individual macerals are not considered in this model. The influence of the maceral concentration is assumed to occur through its effect on the average elemental and functional group composition. If details on macerals are desired then each maceral must be treated as a distinct molecular population with its own functional group composition and molecular weight distribution.

e. **Physical Properties of Molecular Fragments.** The general model has assumed that the vaporization and solubility of the molecular fragments are functions of molecular weight alone. Both properties are expected to depend on functional group composition. Such effects can be included as corrections to the vaporization law and solubility assumptions.

The Depolymerization-Vaporization-Crosslinking (DVC) Subroutine Formulation.

The DVC model has been described in a number of publications (30,31,44-47,50,51). It predicts the tar yield, the tar molecular weight distribution, the char yield, the char molecular weight distribution, the extract yield and the crosslink density. The model had its beginning in a study of polymers representative of structural features found in coal (44). The objective of that study was to develop an understanding of coal pyrolysis by studying a simpler, more easily interpretable system. The polymers were studied in a series of pyrolysis

experiments in which tar amounts and molecular weights were measured. The theory which was developed describes the combined effects of: 1) **depolymerization and hydrogen consumption**; 2) **cross-linking**; and 3) **external transport**. Recently, an expression to describe 4) **internal transport** has been added to the model (33). These processes, which are described below, are incorporated into a computer code which employs a Monte Carlo method for performing the statistical analysis.

Process 1. Depolymerization and Hydrogen Consumption. Bond cleavage in coal is likely to be very complicated, including homolytic cleavage, ipso substitution (46) and hydrogen-transfer induced bond scission reactions (72) for a variety of bond types. However, it has been observed that tar evolution is consistent with a narrow distribution of activation energies (5,6,12), which allows consideration in the model of a single type of bridge (while acknowledging that other types may be present). Also, the rate for tar formation from coal, k_{tar} , (6,13) is in good agreement with the rate, determined for the breaking of ethylene bridges between naphthalene rings, k_B . This kinetic rate, k_B , (46) employs an activation energy which is in agreement with resonance stabilization calculations (73,74) and an overall rate which agrees with previous measurements on model compounds (75). In view of these observations, a single type of bond (ethylene) undergoing homolytic cleavage is assumed for coal as a simple approximation of the complicated behavior.

Bond cleavage is accompanied by the consumption of donatable hydrogens, $H(a)$, to cap free radicals, along with corresponding carbon-carbon double bond formation at the donor site. In the polymers which were studied, the ethylene bridges were identified as a source of donatable hydrogen with the formation of a double bond between the bridge carbons (46,47). The double bond formation was assumed to remove a breakable bond. It should be noted that hydroaromatic groups are also a source of donatable hydrogen with aromatization of the ring. However, for

simplicity, the DVC model assumes all the coal's donatable hydrogens, whether in bridges or in hydroaromatic rings, are in bridges, i.e., $H(al) = (2/28)W_B$. This approximation will produce some error in tar yield since a broken bond in a hydroaromatic ring will not be as effective as a broken bond in a bridge in fragmentating the coal. But this effect will be compensated for, since $H(al)$ is a parameter which is determined for each coal from a selected pyrolysis experiment. $H(al)$ could, in principle, be determined by FT-IR or NMR but not with sufficient accuracy.

The equation describing the disappearance of labile bridges in the char, $W_B(\text{char})$, due to bond breaking and hydrogen donation is,

$$dW_B/dt = -2k_B W_B \quad (1)$$

The value for k_B is taken as the previously determined k_{tar} (6). The rate of decrease of labile bridges is twice the rate of bond breaking since for each broken bond, an additional labile bridge is converted to a non-labile bridge with the donation of hydrogen. By assuming that all the donatable hydrogens are in the labile bridges, the consumption of labile bridges and donatable hydrogens occur simultaneously. The redistribution of hydrogen creates source and loss terms, $dW_i(DVC)/dt$, in the equations for the char functional groups $W_i(\text{char})$, as will be discussed with the FG part of the model (see Eq. 7).

Equation 1 only describes the loss due to bond breaking and hydrogen donation. The loss of labile bridges due to evolution with the tar is computed in the Monte Carlo calculation using the transport equations (Eqs. 3 and 4) discussed below.

Process 2. Crosslinking. Crosslinking reactions are important in describing

the rank and heating rate dependence of the tar molecular weight distributions and yields. While crosslinking reactions were originally included in the DVC model using adjustable parameters for the rate and amount (30,31,46), work has recently been performed to define the reactions which cause crosslinking (33,50,51). Under the assumption that the crosslinking reactions may also release gas species, the molecular weight between crosslinks (or crosslink density) measured by solvent swelling was correlated with the observed evolution of all the major gas species during pyrolysis. Likely candidates were CO₂ formation from carboxyl groups or methane formation from methyl groups. Suuberg et al. (59) also noted that crosslinking in low rank coals is correlated with CO₂ evolution. Both CO₂ and CH₄ forming reactions may leave behind free radicals which can be stabilized by crosslinking. Condensation of hydroxyl groups to form water and an ether link is also a possible reaction.

For a series of chars, the reduction in the volumetric swelling ratio in pyridine was compared with CO₂ evolution for a North Dakota (Beulah) lignite and CH₄ evolution for a Pittsburgh Seam bituminous coal (50). The results are presented in Fig. 2. The abscissa (parameter Z), which is the change in the volumetric swelling ratio (VSR) between coal and char divided by the maximum change is given by:

$$Z = (VSR_{\text{coal}} - VSR_{\text{char}}) / (VSR_{\text{coal}} - VSR_{\text{min}})$$

Z is 0 for coal and 1 for fully crosslinked char. Since the lignite reaches maximum crosslinking before the start of methane evolution and the Pittsburgh Seam bituminous coal evolves little CO₂, correlations can be made separately between crosslinking and CO₂ evolution in the lignite and crosslinking and CH₄ evolution in the Pittsburgh seam bituminous coal. On a molar basis, the evolution of CO₂ from

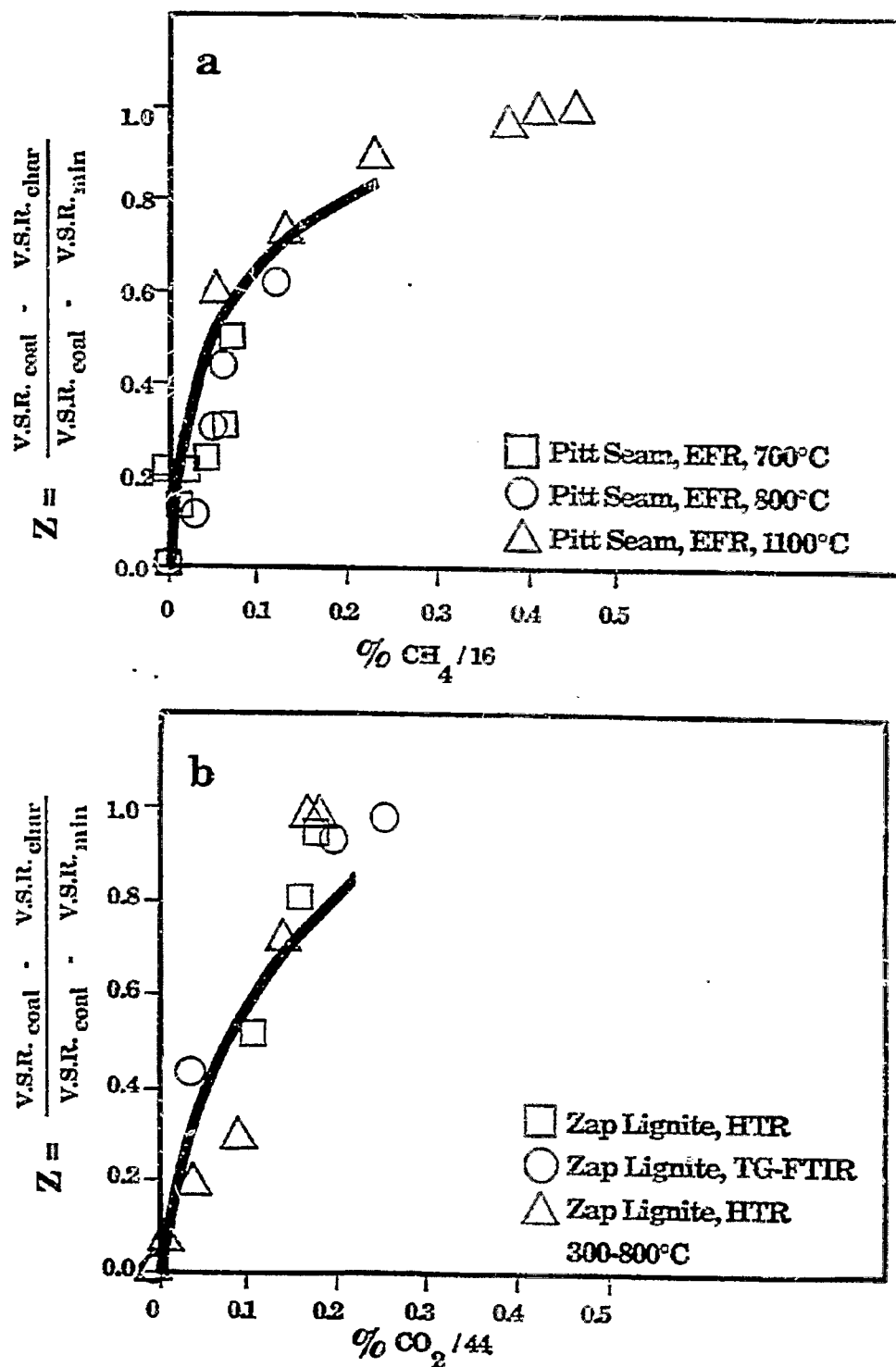


Figure 2. Measured and Calculated Normalized Volumetric Swelling Ratio (VSR), for Coal and Chars. a) Pittsburgh Seam Bituminous Coal Plotted Against the Methane Yield and b) Zap North Dakota Lignite Plotted Against CO₂ Yield. V.S.R._{min} is the Value Achieved when Crosslinking is Complete. The Chars were Prepared in an Entrained Flow Reactor (EFR), a Heated Tube Reactor (HTR), and a Thermogravimetric Analyzer with Evolved Product Analysis by FT-IR (TG-FTIR) Described in Ref. 61.

the lignite and CH₄ from the bituminous coal appear to have similar effects on the volumetric swelling ratio. The results suggest that one crosslink is formed for each CO₂ or CH₄ molecule evolved. No correlation was observed between the volumetric swelling ratio and tar yield for either coal. A correlation with water yield appears valid for the North Dakota (Beulah) lignite, but not for the Pittsburgh Seam bituminous coal.

it therefore appears that a correlation exists between gas evolution and crosslinking, which permits the rates for crosslinking and the number of crosslink sites to be related to rates and yields for gas evolution. The model assumes the following expression for the rate of increase of the number of crosslinks, m per gram of coal

$$\frac{dm}{dt} = N_0 \left[\frac{dW_{CO_2}(\text{gas})/dt}{44} + \frac{dW_{CH_4}(\text{gas})/dt}{16} \right] \quad (2)$$

where the rates, dW_i/dt , of evolution of CO₂ and CH₄ per gram of coal are calculated in the FG subroutine. N_0 is Avogadro's number.

Again, a caution should be added that the reactions which have been assumed must be a gross simplification of a very complicated set of chemical reactions. This is especially true for the crosslinks occurring during methane formation, during which time there is extensive bond breaking and crosslinking accompanying tar formation. The inaccuracy in the description of this higher temperature crosslinking event is one of the present weaknesses in the model.

Process 3. External Transport. The external transport of tars from the particle surface to the bulk gas by vaporization and diffusion through a gas

boundary layer as in the original DVC model (44-47,50,51) is described with the model of Unger and Suuberg (23). However, in the current paper, the modified expression for the vapor pressure law of Suuberg et al. (32) is now used to replace that in the model of Unger and Suuberg. The rate of evolution per gram of coal, $(dn_j/dt)_{ET}$, of oligomers of molecular weight M_j is given by

$$(dn_j/dt)_{ET} = (3/r_0^3 \rho) r D_j X_j^s (P_j/RT) \quad (3)$$

where r is the particle radius assumed to shrink with the cubic root of its mass and r_0 is the initial particle radius, ρ is the particle density, X_j^s is the mole fraction of species of molecular weight M_j in the metaplast at the surface of the particle, P_j is the vapor pressure for oligomers of molecular weight M_j (given by Suuberg et al. (32), D_j is the gas phase diffusivity of species of molecular weight M_j (44), R is the gas constant and T is the particle temperature.

In the previous work, it was assumed that the surface mole fraction, X_j^s , was the same as that in the bulk, X_j^b . That is, mass transport to the surface was not a limiting factor.

Process 4. Internal Transport. When comparing the predictions of the model to available data assuming $X_j^s = X_j^b$ it was found that tar yields were overpredicted when devolatilization occurred at low temperatures. This was observed for either low heating rate experiments (6) or experiments with rapid heating to relatively low temperatures (16). As discussed in the Results Section, it appears that the lower yields were the result of the additional transport limitations within the particle.

For softening coals, the internal transport mechanisms include: i) the transport of tar molecules through the liquid to the surface; ii) the transit of bubbles containing tar from the interior of the particle to the surface; iii) the transport of tars within the liquid to the bubbles; and iv) the stirring action of the bubble evolution. For non-softening coals, transport occurs by; v) convection and diffusion within the pores.

Mechanism i was treated by Suuberg and Sezen (36). The unknown factor is the diffusion coefficient of the tar molecules in the liquid. The detailed modeling of mechanisms ii and iii has been undertaken by several investigators (4,26,37,38). Calculations for mechanism v have also been published (24,25,34,35). The models are complicated and require many assumptions. A common feature of mechanisms iii and v is that tars are transported out of the particle with the light devolatilization products which exit the coal via bubbles or pores. In Ref. 33, the upper limit for this process was calculated. This limit, which occurs when the tars achieve their equilibrium vapor pressure in the evolving gases, can be computed with few assumptions. In this case, the rate of transport, per gram of coal $(dn_j/dt)_{IT}$, for tar component j is proportional to the volume of gases evolved, dV/dt . That is

$$(dn_j/dt) = P_j X_j^b dV/dt (1/RT).$$

The volume of gases is proportional to the number of gas molecules and the temperature. It is inversely proportional to the pressure within the particle, $P_0 + \Delta P$ where P_0 is the ambient pressure and ΔP is the average pressure difference between the surface and the particle's interior. Then

$$dV/dt = \sum_i (dn_i/dt)_{\text{gas}} \frac{RT}{P_0 + \Delta P}$$

where $\sum_i (dn_i/dt)_{\text{gas}}$ is the rate of production per gram of coal of gas components i summed over all gas and light tar species. For gas molecules, dn_j/dt is taken as the rate of production given by the FG model. For light tar molecules dn_j/dt is taken as the total amount transported out of the particle as tar computed in the previous time step. For computational efficiency, the sum has been limited to molecular weights less than 300 amu, since this accounts for over 90% of the volume. Combining the two equations with this approximation gives,

$$(dn_j/dt)_{IT} = P_j X_j^0 \sum_{i < 300} (dn_i/dt)_{\text{gas}} \left[\frac{1}{P_0 + P} \right] \quad (4)$$

ΔP is used as an adjustable parameter which varies with the coal and experimental conditions. For the highly fluid Pittsburgh Seam bituminous coal, in cases where P_0 is one atmosphere or greater, we have considered the upper limit to this rate where $P_0 \gg \Delta P$. Then all the terms in Eq. 4 can be determined by the combined FG-DVC model. This limit coincides with assumptions recently used by Niksa in his FLASHKIN model for Pittsburgh Seam bituminous coal (76).

While $\Delta P = 0$ appears to be a good approximation for fluid coals at one atmosphere or more, $\Delta P > 0$ is expected for some coals and situations. ΔP is proportional to the coal's viscosity and so, will become important for less fluid coals. ΔP is also important when P_0 is small, for large particles and when the heating rates are very high.

Two possibilities have been considered for combining the internal and external transportation. In an earlier publication (33), the internal transport term and external transport term (with $X_j^s = X_j^b$) were assumed to be in series. Then the transport was controlled by the smaller term. The internal transport term was the smaller for all pyrolysis cases that were considered and so it dominated. In fact, calculations performed neglecting the external transport limitation were almost identical to those made assuming the two terms to be in series.

Alternatively, a case can be made that the total transport should be the sum of Eqs. 3 and 4. The reasoning is that internal transport assumes the tars to be in equilibrium with the escaping light gases. It is more likely that this mechanism will transport the tars to the ambient gas than to the surface. In this case, the mechanism considered in Eq. 4 transports the tars away from the surface in parallel with the surface evaporation and gas diffusion considered in Eq. 3.

If the two terms are taken in parallel, it is again obvious that $X_j^s = X_j^b$ is a bad assumption. Not having a good method to determine X_j^s , calculations were made assuming that the external transport term can be neglected i.e.,

$$(dn_i/dt)_{\text{total}} = (dn_i/dt)_{IT}.$$

This provides an excellent fit to the data for 50 μm diameter particles.

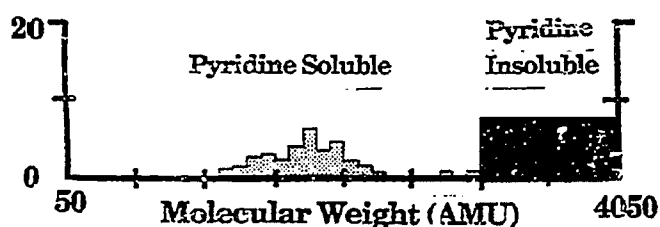
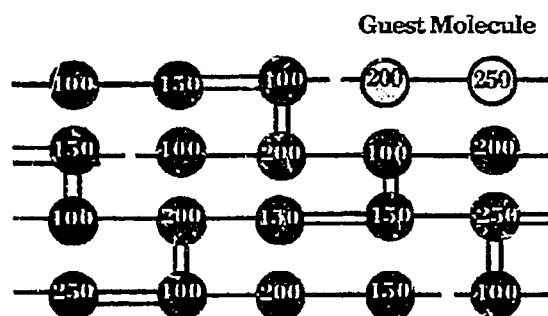
Therefore, for either parallel or series combinations of the transport terms, it appears best to neglect the external transport. It is likely that the external transport term will be increasingly important for smaller particles, but this will require better knowledge of the liquid phase diffusion coefficient, (mechanism i) and the stirring action of bubbles (mechanism iv). The relative importance of the

various internal and external transport mechanisms is the subject of on-going research.

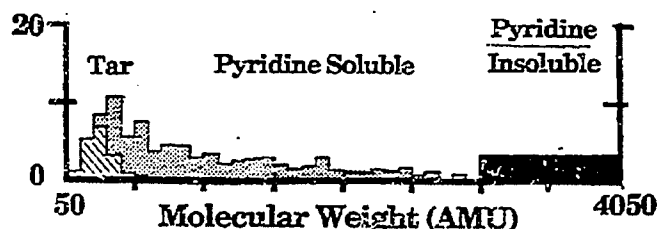
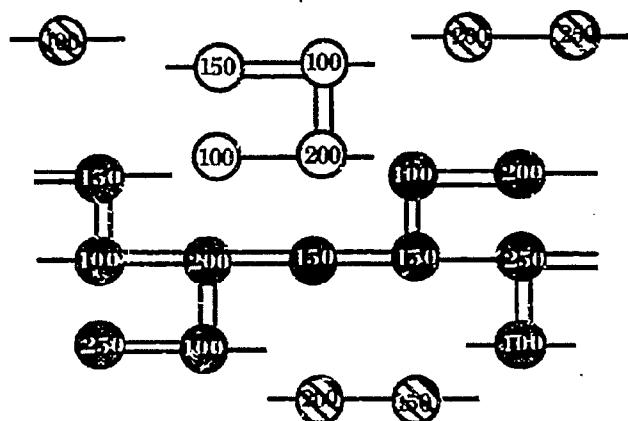
Schematic Representation of DVC Model.

In the current DVC model, the parent coal is represented as a two-dimensional network of monomers (condensed ring clusters) linked by strong and weak bridges as shown in Fig. 3a. The monomers are linked to form unbranched oligomers of length " ℓ " by breakable and non-breakable bridges (shown as horizontal single or double lines, respectively in Fig. 3a). The monomers are represented by circles with molecular weights shown in each circle. The molecular weight distribution of the monomers is assumed to be Gaussian and is described by two parameters, M_{avg} (mean) and σ (standard deviation). The breakable bridges (assumed to be ethylene) are represented by single lines, the unbreakable bridges by double lines. " m_0 " crosslinks per gram are added (as vertical double lines in Fig. 3a) to connect the oligomers of length ℓ so that the molecular weight between crosslinks, M_c , corresponds to the value reported in the literature (77) for coals of similar rank. The crosslinks form the branch points in the macromolecule. Unconnected "guest" molecules (the extract yield) are obtained by choosing the value of ℓ . A large value of ℓ will mean that a completely connected macromolecule will be formed when even a small number of crosslinks are added, leaving no extractable material. For smaller values of ℓ some of the oligomers will be unattached after the crosslinks are added and these are the guest molecules. The number of ethylene bridges, N_b , (two donatable hydrogens per bridge) is chosen to obtain the appropriate value for total donatable hydrogen (i.e., to fit a selected laboratory pyrolysis experiment). The remainder are non-breakable bridges whose carbons are counted with the aromatics carbons.

a. Starting Molecule



b. During Tar Formation



c. Char Formed

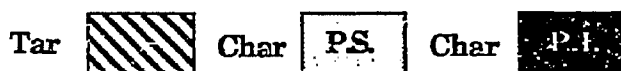
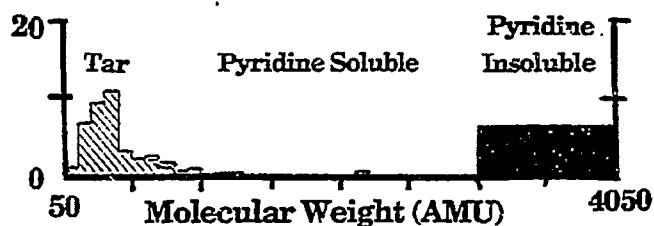
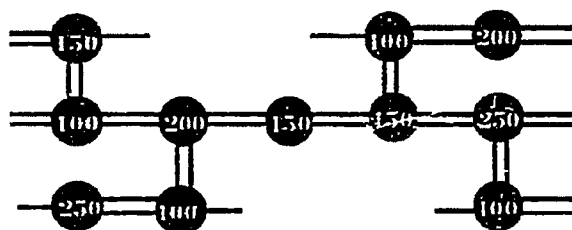


Figure 3. Representation of Coal Molecule in the DVC Simulation and Corresponding Molecular Weight Distribution. In the Molecule, the Circles Represent Monomers (ring clusters and peripheral groups). The Molecular Weight Shown by the Numbers is the Molecular Weight of the Monomer Including the Attached Bridges. The Single Line Bridges are Breakable and can Donate Hydrogen. The Double Line Bridges are Unbreakable and do not Donate Hydrogen. The Molecular Weight Distribution of the Coal, Tar, and Chars are Shown as a Histogram at the Right. The Histogram is Divided into Tar and Char with Pyridine Soluble and Insoluble Fractions. The Area Under the Histogram Corresponds to the Weight Percent of the Oligomers.

The parameters M_c , ℓ , M_{avg} and σ determine the molecular weight distribution of oligomers in the starting coal molecule. A histogram showing the distribution created by randomly picking monomers to form oligomers of length ℓ and randomly crosslinking them to achieve an average molecular weight between crosslinks, M_c , is presented at the right of Fig. 3a. The distribution is divided into a pyridine soluble portion below 3000 AMU (light shading) and a pyridine insoluble portion above 3000 AMU (dark shading).

Figure 3b shows the molecule during pyrolysis. The rates for bond breaking and crosslinking are from the FG model and are the same for all coals and all experiments. Some bonds have broken, other bonds have been converted to unbreakable bonds by the abstraction of hydrogen to stabilize the free radicals and new crosslinks have been formed. To determine the change of state of the computer molecules during a time step, the number of crosslinks formed is determined using the FG subroutine, and passed to the DVC subroutine. These crosslinks are distributed randomly throughout the char, assuming that the crosslinking probability is proportional to the molecular weight of the monomer. Then the DVC subroutine breaks the appropriate number of bridging bonds and calculates the quantity of tar evolved for this time step using the internal and external transport equations. The result is the coal molecule representation and the molecular weight distributions shown in Fig. 3b. The lighter "tar molecules", which leave the particle according to the transport equations, are shown as cross hatched. A fraction of the donatable hydrogen is used to stabilize the free radicals formed by bridge breaking, creating two new methyl groups per bridge and the same fraction of breakable bridges is converted into (unbreakable) double-bonds.

Figure 3c shows the final char which is highly crosslinked with unbreakable bonds and has no remaining donatable hydrogen. The histogram now shows only tar and pyridine insoluble fractions. The extractables have been eliminated by tar formation and crosslinking.

The output of the DVC subroutine is the molecular weight distribution in the coal, its time dependent transformation during devolatilization and the evolution of tar determined by the transport of the lighter components.

Selection of DVC Parameters.

The DVC composition parameters employed for a Pittsburgh Seam coal and North Dakota lignite are summarized in Table I. The FG composition parameters and the kinetic parameters, which are fixed for all coals and experiments, are presented in Table II. In Table I, there are eleven independent composition parameters. Three parameters are fixed, the molecular weight of the labile bridges, M_C , the non-labile bridges, M_{NL} , and the pyridine extractable limit, M_{PS} .

Eight parameters are coal specific, (i.e., fixed for each coal, for all conditions) and must be determined by some measurement. M_C and ℓ are determined experimentally for each coal by the measured molecular weight between crosslinks and the pyridine extract yield, respectively. The weight fraction of carbon in nuclei and non-breakable bridges, W_N , is obtained from the FG model and is equal to the non-volatile carbon. This value is, in principle, determined for each coal from a single pyrolysis experiment. In practice, several experiments are performed. The number of potential crosslink sites, $m(CO_2)$ and $m(CH_4)$, are proportional to the total yield of CO_2 and the total yield of CH_4 , respectively. W_B , M_{avg} , and σ are determined by using the model to fit selected pyrolysis

Table I - Coal Structure Parameters for DVC Subroutine.

Parameter	Symbol	Parameter Determination				Parameter Values	
		Fixed	Coal Specific-Determined	Adjustable	Dependent*	Pittsburgh Seam	Zap Ligite
Concentrations							
Weight Fraction of Labile Bridges	W_B		from Tar Yield in a Pyrolysis Experiment			0.091	0.082
Weight Fraction of Nuclei (ring clusters)*	W_N		from FG Model			0.562	0.440
Weight Fraction of Peripheral Groups (sources for gases)*	W_P				by Difference	0.344	0.478
Total						1.000	1.000
Structure Parameters							
Weight Fraction of Donatable Hydrogens H(al) [†]	H(al)				(278) W_B	0.0007	0.0059
Oligomer Length (#monomers/oligomer)			from Extract Yield			7	10
Molecular Weight Between Crosslinks	M_C		from Solvent Swelling (literature values)			2000	1400
Number of Labile Crosslink Sites per Monomer*	m_D				M_{avg}/M_C	0.0028	0.119
Number of Potential CO ₂ Crosslink Sites per Monomer	$m(CO_2)$		from FG Model			.970	0.892
Number of Potential CH ₄ Crosslink Sites per Monomer	$m(CH_4)$		from FG Model			1.063	0.875
Molecular Weights							
Molecular Weight of Labile Bridges	M_L	29				29	29
Molecular Weight of Monomers	$M_{avg} (\sigma)$		from FIMS or NMR			256, (250)	253, (250)
Molecular Weight of Non-Labile Bridges	M_{NL}	20				20	26
Molecular Weight of Pyridine Solubles	M_{PS}	3000				3000	3000
Other							
Internal Pressure	ΔP				for Each Coal, Particle Size and Reaction Rate	0-0.2 atm	1-10 atm

* Carbon in Aromatic Rings plus Non-Labile Bridges.

† Dependent Parameters are Calculated from the Independent Parameters.

Table II - Kinetic Rate Coefficients and Species Composition Parameters for FG Subroutine.

composition parameters	gas	primary functional group source	rate equation ^a	Pittsburgh No. 8 bituminous coal	North Dakota Zap Lignite
C				0.821	0.665
H				0.056	0.048
N				0.017	0.011
S(organic)				0.024	0.011
O				0.082	0.265
total				1.000	1.000
Y ₁ ^p	CO ₂ extra loose	carboxyl	k ₁ = 0.81E+13 exp(-22500±1500/T)	0.000	0.065
Y ₂ ^p	CO ₂ loose	carboxyl	k ₂ = 0.65E+17 exp(-33850±1500/T)	0.007	0.030
Y ₃ ^p	CO ₂ tight		k ₃ = 0.11E+16 exp(-38315±2000/T)	0.005	0.005
Y ₄ ^p	H ₂ O loose	hydroxyl	k ₄ = 0.22E+16 exp(-3000±1500/T)	0.012	0.062
Y ₅ ^p	H ₂ O tight	hydroxyl	k ₅ = 0.17E+14 exp(-32700±1500/T)	0.012	0.033
Y ₆ ^p	CO ether loose		k ₆ = 0.14E+19 exp(-40000±6000/T)	0.050	0.060
Y ₇ ^p	CO ether tight	ether O	k ₇ = 0.15E+16 exp(-40500±1500/T)	0.021	0.038
Y ₈ ^p	HCN loose		k ₈ = 0.17E+14 exp(-30000±1500/T)	0.009	0.007
Y ₉ ^p	HCN tight		k ₉ = 0.69E+13 exp(-42500±4750/T)	0.023	0.013
Y ₁₀ ^p	NH ₃		k ₁₀ = 0.12E+13 exp(-27300±3000/T)	0.000	0.001
Y ₁₁ ^p	CH _x aliphatic	H(al)	k ₁₁ = 0.84E+15 exp(-30000±1500/T)	0.207	0.102
Y ₁₂ ^p	methane extra loose	methoxy	k ₁₂ = 0.84E+15 exp(-30000±1500/T)	0.000	0.000
Y ₁₃ ^p	methane loose	methyl	k ₁₃ = 6.75E+14 exp(-30000±2000/T)	0.020	0.017
Y ₁₄ ^p	methane tight	methyl	k ₁₄ = 0.34E+12 exp(-30000±2000/T)	0.015	0.009
Y ₁₅ ^p	H aromatic	H(ar)	k ₁₅ = 0.10E+15 exp(-40500±6000/T)	0.013	0.017
Y ₁₆ ^p	methanol		k ₁₆ = 0.00E+00 exp(-30000±0/T)	0.000	0.000
Y ₁₇ ^p	CO extra tight	ether O	k ₁₇ = 0.20E+14 exp(-45500±1500/T)	0.020	0.090
Y ₁₈ ^p	C nonvolatile	C(ar)	k ₁₈ = 0	0.562	0.440
Y ₁₉ ^p	S organic			0.024	0.011
X ^p	tar		k _B = k _T = 0.86E+15 exp(-27700±1500/T)	1.000	1.000

a. The rate equation is of the form $k_n = k_0 \exp(-(E/R) \pm (\sigma/R)/T)$, with k_0 in s⁻¹, E/R in K, and σ/R in K. The σ designates the spread in activation energies in a Gaussian distribution.

experiments. The value of W_B is adjustable to fit the tar yield or total volatile yield from one or two selected experiments. In principle, W_B could be measured by FT-IR or NMR but not with sufficient accuracy for this highly sensitive parameter. The values of M_{avg} and σ are chosen based on FIMS analysis of the coal. M_{avg} can be determined from the average cluster size determined by NMR (78,79). The value of 256 chosen for both the lignite and bituminous coal is in reasonable agreement with these reported by Solum, et al. (79), 290 for Zap and 300 for the Pittsburgh Seam coal.

One parameter, ΔP is adjustable and can vary with each type of experiment. For fluid coals at pressures above one atmosphere, $\Delta P \approx 0$. For low external pressures, less fluid coals, large particles or high heating rates, $\Delta P > 0$.

There are three dependent parameters which are computed from the other parameters, the weight fraction of peripheral groups, W_p , the donatable hydrogen, $H(al)$, and the number of initial crosslink sites per monomer, m_0 .

Functional Group (FG) Model Formulation.

The Functional Group (FG) model has been described in a number of publications (5,6,11-13). It permits the detailed prediction of the composition of volatile species (gas yield, tar yield and tar functional group and elemental composition) and of char (elemental and functional group composition). It employs coal independent rates for the decomposition of individual assumed functional groups in the coal and char to produce gas species. The ultimate yields of each gas species are related to the coal's functional group composition. Tar evolution is a parallel process which competes for all the functional groups in the coal. In the original FG model, the potential tar forming fraction of the coal, X^0 , was an input

parameter which was adjusted for each coal and type of experiment. In the combined FG-DVC model, the DVC subroutine provides this parameter.

Schematic Representation of FG Model.

The mathematical description of the Functional Group pyrolysis model has been presented previously (5,6,11-13). The evolution of tar and light gas species provides two competing mechanisms for removal of a functional group from the coal: evolution as a part of a tar molecule and evolution as a distinct gas species. This process is shown schematically in Fig. 4. To model these two paths, with one path yielding a product which is similar in composition to the parent coal, the coal is represented as a rectangular area with X and Y dimensions. As shown in Fig. 4a, the Y dimension is divided into fractions according to the chemical composition of the coal. Y_i^0 represents the initial fraction of a particular component (carboxyl, aromatic hydrogen, etc.) and the sum of the Y_i^0 's equal one. The evolution of each component into the gas (carboxyl into CO_2 , aromatic hydrogen into H_2 , etc.) is represented by the first-order diminishing of the Y_i dimension, $dY_i/dt = -k_i Y_i$.

The X dimension is divided into char, X, and tar, (1-X); initially $X = 1$. The evolution of the tar is represented by the decreasing of the X dimension, dX/dt , computed in the DVC subroutine as

$$\frac{dX}{dt} = - \sum_j (dn_j/dt)_{TOT} M_j / M_0$$

The fractional amount of a particular functional group component in the char is

$$W_i(\text{char}) = X \cdot Y_i$$

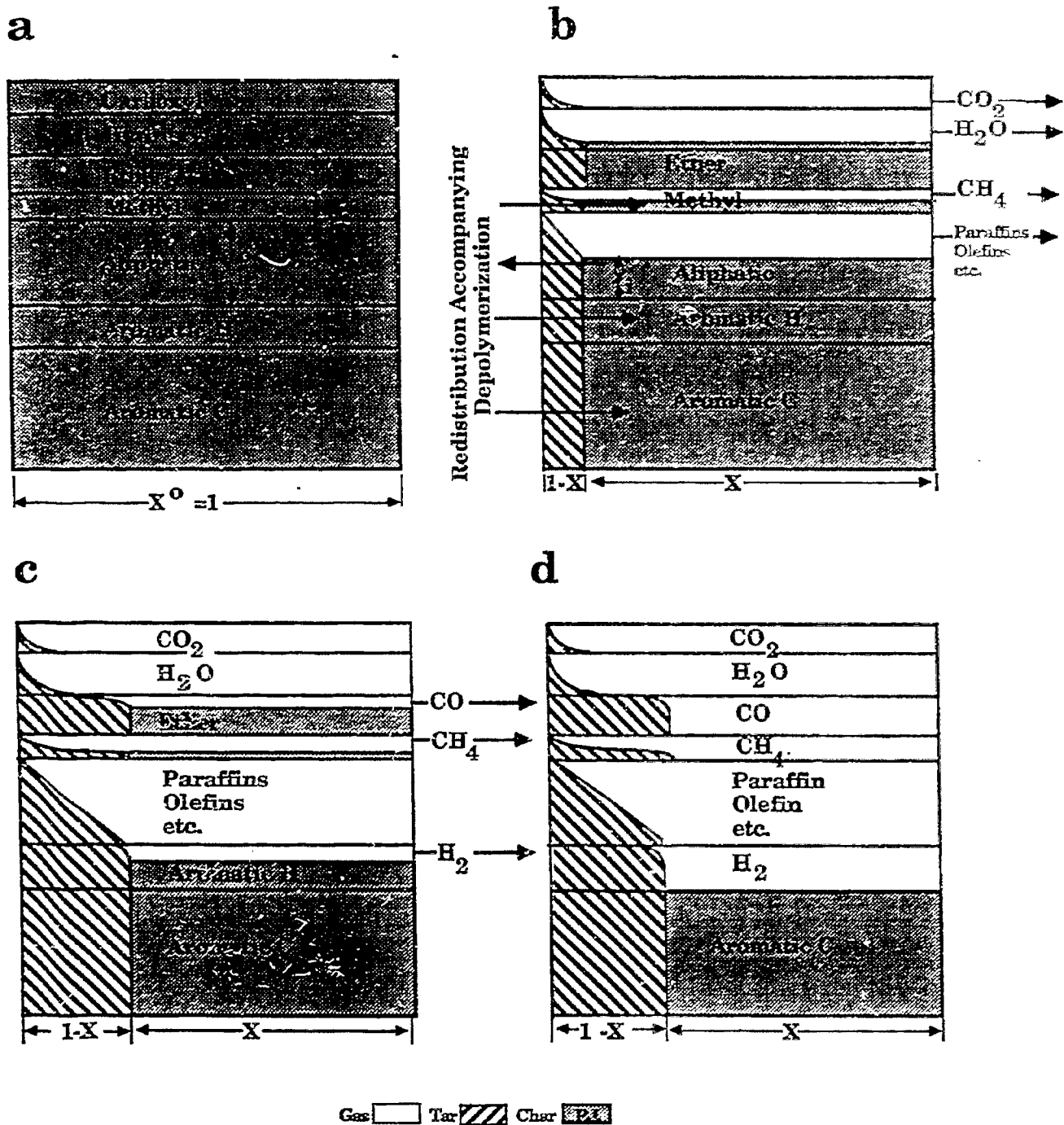


Figure 4. Schematic Representation of Functional Group (FG) Model.
 a) Initial Coal Composition, b) During Tar Formation, c) Completion of Tar Formation, and d) Completion of Devolatilization.

and the amounts in the gas and tar may be obtained by integration with respect to time starting from $t = 0$:

Secondary reactions such as further decomposition of aliphatic species to form olefins, acetylene, and soot modify the basic equations. Some of these have been described elsewhere (6). These types of secondary reactions are not considered in the current paper.

Figure 4a shows the initial state of the coal. Values for Y_i^0 are obtained from elemental analysis and FT-IR analysis of the raw coal, or from analysis of the products of one or two selected pyrolysis experiments. Figure 4b shows the initial stage of devolatilization, during which the most volatile components, H_2O , CO-loose, and CO_2 evolve from the hydroxyl, ether-loose, and carboxyl groups, respectively, along with aliphatics and tar. At a later stage (Fig. 4c) CO-tight, HCN and H_2 are evolved from the ether-tight, ring nitrogen, and aromatic hydrogen. Figure 4d shows the final state of the char, tar and gas.

The evolution of gas and the composition of the char and tar are then described mathematically as follows:

Process 5. Gas Formation. The evolution of each gas species is assumed to be a first order reaction,

$$dW_i(\text{gas})/dt = k_i W_i(\text{char}) = k_i X Y_i \quad (5)$$

where, $dW_i(\text{gas})/dt$ is the rate of evolution of species i into the gas phase, k_i is a distributed rate for species i and $W_i(\text{char})$ is the functional group source remaining in the char. The concept of the distributed rate was introduced by Pitt (80) and subsequently employed by Rennhack (81) and Anthony et al. (22) to describe

weight loss. Hanbaba et al. (82), Juntgen and van Heek (23), Weimer and Ngan (9) and Solomon et al. (12) employed distributed rates for individual species. In the FG subroutine, k_i is given by an Arrhenius expression $k_i = k_0 \exp(-(E_i \pm \sigma_i)/RT)$ where $\pm \sigma_i$ indicates that a Gaussian distribution is employed to describe the product sources, $W_i(E_i)$, as a function of the activation energies E_i (5,9,12,22). $W_i(E_i) = (W_0/\sigma_i \sqrt{2\pi}) \exp(-(E_i - E_0)^2/2\sigma_i^2)$. E_0 is the average activation energy and σ_i is the width of the Gaussian distribution.

Note that $W_i(\text{char})$ also is decreased by its evolution with the tar.

Process 6. Tar Formation. The tar composition is tracked by summing the functional group contributions evolved with the tar. The rate of evolution of each contribution is:

$$dW_i(\text{tar})/dt = -(dX/dt)Y_i \quad (6)$$

where $dW_i(\text{tar})/dt$ is the rate of evolution of each functional group component with the tar.

Process 7. Char Formation. The change in the i th char pool, $W_i(\text{char})$, is computed by summing the losses to the gas and tar and the redistributions determined in the DVC subroutine,

$$dW_i(\text{char})/dt = -dW_i(\text{gas})/dt - dW_i(\text{tar})/dt + dW_i(\text{DVC})/dt \quad (7)$$

where $dW_i(\text{DVC})/dt$ includes the source and loss terms from the DVC model, given by $(30/28)k_B W_B$, $(2/28)k_B W_B$, $(24/28)k_B W_B$ and $-2k_B W_B$ for methyl, aromatic H, aromatic C, and labile bridge functional groups, respectively.

The general rates and specific composition parameters for Pittsburgh Seam coal and North Dakota lignite are presented in Table II.

Schematic and Execution of FG-DVC Model.

Figure 5 presents a schematic of the linked model for a simple case of only one gas species. The combined model connects the upper (DVC portion) and lower (FG portion) parts of Figs. 5a-5d. The model is initiated by specifying the Functional Group composition parameters (w_B , w_N and, in this case, only one gas species parameter, w_p) and the coal structure parameters (starting oligomer length, ℓ , number of added crosslinks, m_0 , and the monomer molecular weight distribution parameters, M_{avg} and σ). The starting molecular weight distribution of oligomers is presented at the top of Fig. 5a. The monomers are assumed to have the average elemental and functional group composition given by the FG parameters. The functional groups are divided into pyridine soluble and pyridine insoluble parts. Each computer simulation considers coal to consist of a network made from 2100-2400 monomers.

Once the starting distribution of oligomers in the coal is established, it is then subjected to a time-temperature history made up of a series of isothermal time steps. Each time step is chosen so the temperature rise in each step does not exceed a fixed maximum. During each step, the gas yields, elemental composition and functional group composition are computed using the FG subroutine. The CO_2 and CH_4 yields are used to determine the number of new crosslinks to be randomly added to the molecule. The molecular weight distribution, the escape of tar molecules and the re-distribution of hydrogens and carbons from the labile groups is computed with the DVC subroutine. Figure 5b illustrates tar formation simultaneous with gas formation. The labile bridges are either evolved with the tar, converted to methyl groups (and thus added to the peripheral groups) or

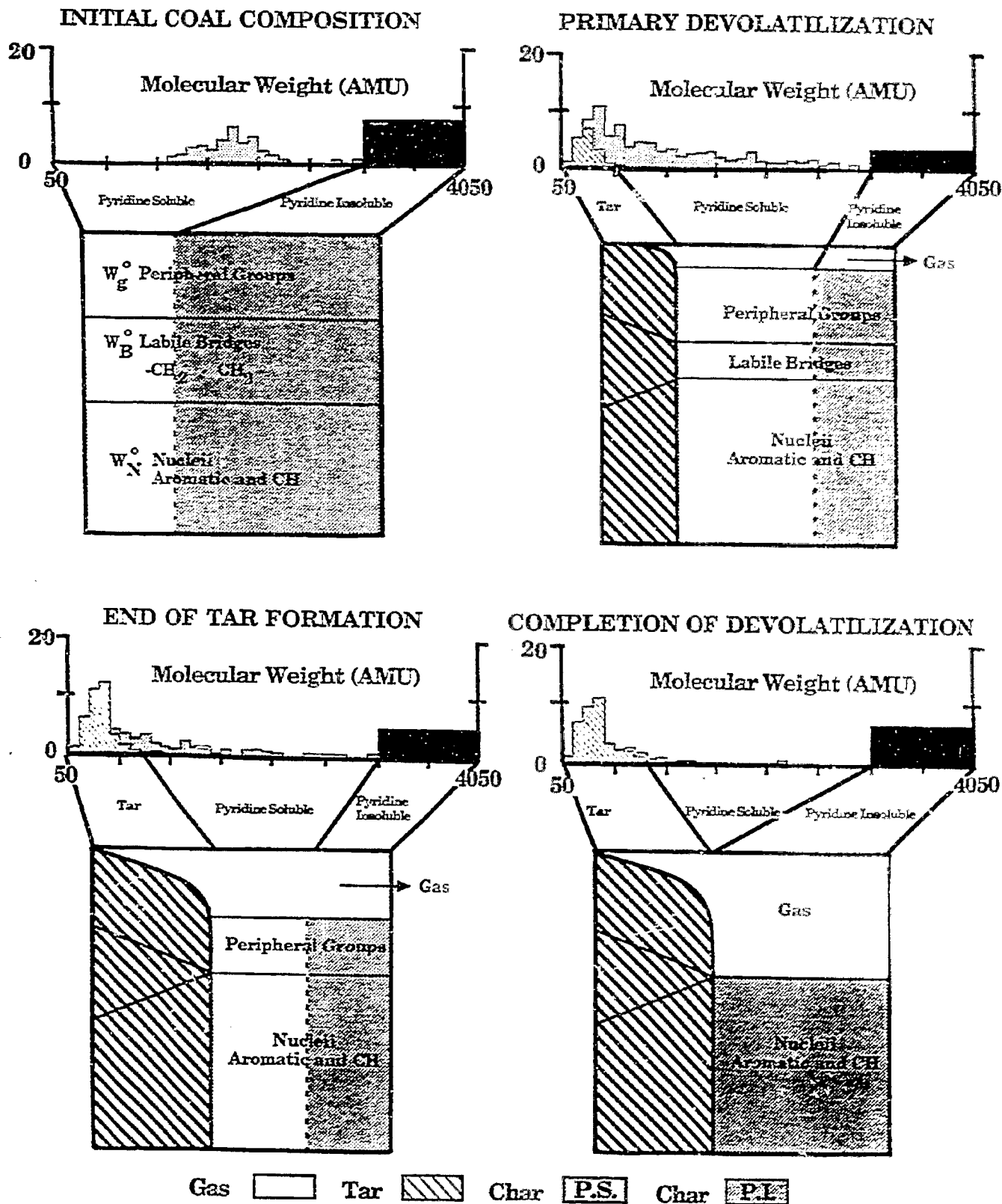


Figure 5. Schematic Representation of the FG-DVC Model Combining the DVC and FG Subroutines. The FG Subroutine is Illustrated for a Single Gas Species Only. The Area Under the Histogram Corresponds to the Weight Percent of the Oligomers.

converted to unbreakable bridges (and thus added to aromatic and CH groups). Tar formation is complete (Fig. 5c) when all the labile bridges are consumed. Devolatilization is completed (Fig. 5d) when all volatile functional groups (in this case the single gas species represented as peripheral groups) are removed from the char.

The model has been programmed in Fortran 77 and runs on the Sun Microsystems 3/260 and 3/50 computers. Run times on a Sun 3/260 are between 83 and 550 sec/simulation for 2100-2400 monomers. A streamlined version of the code designed to run as a subroutine in a comprehensive combustion or gasification reactor simulation employs from 400 to 800 monomers and requires approximately 10 sec/simulation for the pyrolysis of a single particle.

Summary of FG Subroutine Assumptions.

(a) Light gas species are formed from the decomposition of specific functional groups with rate coefficients which depend on the functional group but are independent of coal rank. The evolution rate is first order in the remaining functional group concentration in the char. The rates follow an Arrhenius expression with a Gaussian distribution of activation energies (5,12,22).

(b) Simultaneous with the production of light gas species, is the thermal cleavage of bridge structures in the coal to release molecular fragments of the coal which consist of a representative sampling of the functional group ensemble. These fragments may be transported out of the coal particle to form tar. The instantaneous tar yield is given by the DVC subroutine.

(c) Under conditions where pyrolysis products remain hot (such as an entrained flow reactor), pyrolysis of the functional groups in the tar continues at the same rates used for functional groups in the char, (e.g., the rate for methane formation from methyl groups in tar is the same as from methyl groups in the char).

Summary of DVC Subroutine Assumptions.

(d) The oligomer length, \mathcal{L} , the number of crosslinks, m_0 , and the fraction of labile bridges, W_B , are parameters of the model, chosen to be consistent with the coal's measured extract yield, crosslink density and volatile yield in selected calibration experiments.

(e) The molecular weight distribution is adjusted so that the model predictions fit the observed molecular weight distribution for that coal, measured by pyrolysis of the coal (in vacuum at 3°C/min to 450°C) in a FIMS apparatus (60). Molecular weights 106, 156, 206, 256, 306, 356 and 406 (which are 1,2,3,4,5,6 and 7 aromatic ring compounds with two methyl substituents) are considered as representative of typical monomer molecular weights.

(f) During pyrolysis, the breakable bonds are assumed to rupture randomly at a rate $k_B = k_{tar}$, described by an Arrhenius expression with a Gaussian distribution of sources as a function of activation energies. Each rupture creates two free radicals which consume two donatable hydrogens to form two new methyl groups and convert two more donatable hydrogens to two aromatic CH groups. Oxymethylene bridges, which may be important for low rank coals, have not been modeled although a second class of labile bridges could easily be added.

(g) All the donatable hydrogens are assumed to be located in the labile bridges. Two donatable hydrogens are available at each bridge. The consumption of the donatable hydrogen converts the bridge into an unbreakable bridge by the formation of a double bond. The unbreakable bridges are included in the aromatic hydrogen and aromatic carbon functional groups.

(h) Tar formation continues until all the donatable hydrogens are consumed.

(i) During pyrolysis, additional unbreakable crosslinks are added at a rate determined by the evolution of CH_4 and CO_2 . One crosslink is created for each evolved molecule. The rates of CH_4 and CO_2 evolution are given by the FG subroutine.

(j) The crosslinks are distributed randomly, with the probability of attachment on any one monomer being proportional to the molecular weight of the monomer.

(k) Tar molecules are assumed to vaporize from the surface of the coal particle (or into bubbles) with a molecular weight and temperature dependence based on the vapor pressure correlation of Suuberg et al. (32). The external transport model is based on the surface evaporation model of Unger and Suuberg (23).

(l) To describe internal transport, a simple empirical expression (Eq. 4) is used to describe both bubble transport in softening coals and convective transport through pores in non-softening coals. The tar is assumed to be transported at its equilibrium vapor pressure in the light gas species. The pressure increase which drives the transport within the particle, ΔP is between 0 and 0.2 atm for the

bituminous coal and between 0 and 10 atm for the lignite, depending on the experimental conditions.

(m) Extractable material (in boiling pyridine) in the char is assumed to consist of all molecules less than 3000 AMU. This limit can be adjusted depending on the solvent and extraction conditions.

(n) The molecular weight between crosslinks, M_c , is computed to be the total molecular weight in the computer molecule divided by the total number of crosslinks. This assumption will underestimate M_c since broken bridges are not considered.

RESULTS

The model predictions have been compared to the results obtained from a number of experiments on the pyrolysis of a Pittsburgh Seam coal (6,7,16,22) and a North Dakota (Beulah, Zap) lignite (6,51). The coal composition and kinetic parameters are presented in Tables I and II. It should be noted that different samples of Pittsburgh seam coal from different sources were employed. While the elemental compositions were similar, extract yields varied depending on the sample source. The oligomer length in Table I was chosen to fit an extract yield of 30% for the Pittsburgh Seam coal and 1% for the lignite. Comparisons are considered for gas yields, tar yields, tar molecular weight distributions, extract yields and volumetric swelling ratios.

Volatile Yields. Extensive comparisons of the FG model with gas yields have been presented previously for high and low heating rate devolatilization experiments (5,6,11-13). The evolution of gases for the combined model is similar to results of the FG model and will not be repeated here. There is good agreement

between the measured and predicted results. The Functional Group parameters and the kinetic rates used for this work for the Pittsburgh Seam coal and North Dakota (Zap) lignite are principally those determined previously and published in Ref. 6. The methane parameters for the Pittsburgh Seam coal were, however, adjusted (methane X-L = 0.0, methane-L = 0.02, methane-T = 0.015, unchanged) to better match yields of Refs. 5,6 and 7 (see Fig. 20c in Ref. 6). Also note that the CH_x -aliphatic rate in Ref. 6 applies to the observed gas species (paraffins, olefins, C_2H_6 , C_2H_4) only. The aliphatic material in the labile bridge part of the aliphatic groups is assumed to be made up of bridges which volatilize only when attached to a tar molecule (i.e., $k_i = 0$). Also, the rate for CO_2 -loose has been adjusted to improve the predictions of the change in tar molecular weight distributions and yield with heating rate. The predictions of gas yield due to this change have not been changed noticeably. The predicted values of X^0 from the DVC subroutine vary with heating rate and final temperature and are in good agreement with the values of X^0 used in the original FG model.

Extract Yields. Figure 6 compares the FG-DVC predictions to the data of Fong et al. (16) on total volatile yield and extract yield as a function of temperature in pyrolysis at 0.85 ATM. The experiments were performed in a heated grid apparatus at heating rates of approximately 500°C/sec, with variable holding times and rapid cool down. The predictions at the two higher temperatures (Figs. 6c and 6d) are in excellent agreement with the data.

The initial predictions for the two lower temperature cases, which neglected internal transport limitations, were not good. The dashed line in Fig. 6a shows the predicted yield in the absence of internal transport limitations (i.e., $(dn_j/dt)_{IT} = 0$ and with $X_j^s = X_j^b$ in Eq. 3). The predicted ultimate yield is clearly too high. The data suggest that the low yields are not a result of

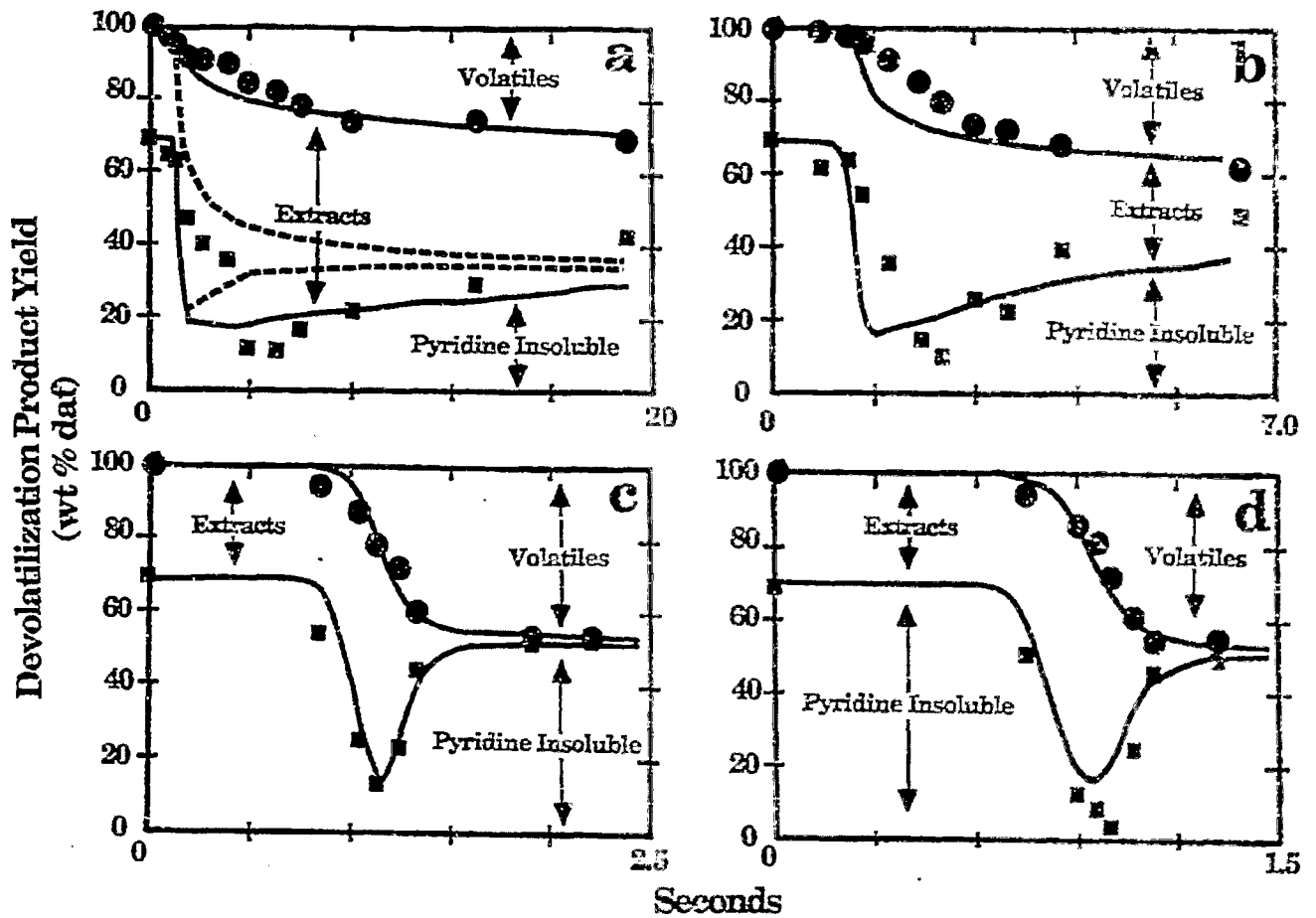


Figure 6. Comparison of FG-DVC Model Predictions with the Data of Fong et al. (16) (symbols) for Pittsburgh Seam Coal. a) 813 K @ 470 K/s, b) 858 K @ 446 K/s, c) 992 K @ 514 K/s, and d) 1018 K @ 640 K/s. $P = 0.85$ atm. The Solid Line Assumes Transport by Eq. 4 ($\Delta P = 0$ atm) and no External Transport. The Dashed Line in 6a Shows the Predicted Yield Assuming $\chi_i^s = \chi_i^b$ in Eq. 3 and no Internal Transport Limitations.

unbroken bonds (which would result from a lower bond breaking rate, k_B), since the extract yields at low temperatures are equivalent to those at the higher temperatures. The coal molecule thus appears to be well decomposed, the low yields resulting from poor transport out of the coal. This suggested an additional transport limitation in getting molecules to the surface, so $X_j^s = X_j^b$ appears to be a bad assumption.

Equation 4 was employed for the internal transport rate and surface evaporation by Eq. 3 was assumed to be unimportant ($X_j^s = 0$). Then, W_B had to be slightly readjusted from 0.096 in Ref. 50 to 0.094 to match the 1018 K case. This new value of W_B was used for subsequent cases. The predictions with this assumption are the solid lines in Fig. 6. The internal transport limitation is most important when pyrolysis occurs at low temperatures and $\sum \text{light } dn_i/dt$ in Eq. 4 is small.

There still is a discrepancy between the prediction and the data at early times for the two lower temperature cases (Figs. 6a and 6b). While it is possible that the rate k_B for bond breaking is too high, adjustment of this rate alone would significantly lower the extractable yield, since the lower depolymerization rate is closer to the methane crosslinking rate. In addition, both the methane and depolymerization rates appear to be in good agreement with the data at even lower temperatures (6). Another possibility is that the coal particles heat more slowly than the nominal temperatures given by Fong et al. (16). Such an effect could be caused by having some clumps of particle which would heat more slowly than isolated particles, by reduction in the convective heat transfer due to the volatile evolution (blowing effect), or by endothermic tar forming reactions. A firm conclusion as to the source of this remaining discrepancy cannot be drawn without further investigation.

It is also seen in Figs. 6a and 6b that the crosslinking rate is higher than predicted. This can be due to other crosslinking events not considered. These possibilities are currently under investigation.

Crosslink Density. To examine the effect of coal rank on crosslinking, the volumetric swelling ratios (VSR) for North Dakota (Beulah, Zap) lignite and Pittsburgh Seam bituminous coal were measured as a function of temperature at $0.5^{\circ}\text{C}/\text{sec}$. The VSR can be related to the crosslink density (77). The swelling data are plotted in Fig. 7a as $1-Z$, where Z is the change in VSR between coal and char normalized by the maximum change. For coal, Z is 0 and for completely crosslinked char, Z is one. While the weight loss profiles of the two samples look similar at $0.5^{\circ}\text{C}/\text{sec}$, the swelling behaviors in Fig. 7a are quite different. The Pittsburgh Seam coal starts to crosslink during tar evolution and the Beulah lignite crosslinks well before tar evolution. Similar results have been reported by Suuberg et al. (59) who also suggested a correlation between crosslinking in lignites and CO_2 evolution. The coals which undergo early crosslinking are less fluid, produce less tar and produce lower molecular weight tar compared with coals which don't experience early crosslinking (30,31,44).

As discussed previously, under the assumption that the crosslinking reactions may also release gas species, the VSR was correlated with the observed evolution of gas species during pyrolysis. Correlations presented in Fig. 2 show that on a molar basis, the evolution of CO_2 from the lignite and CH_4 from the bituminous coal appear to have similar effects on the VSR. Reactions which form these gases, leave behind free radicals which can be stabilized by crosslinking.

Assuming that one crosslink is formed for each CO_2 or CH_4 evolved from the char, the FG-DVC model predictions are presented as the lines in Figs. 2 and 7a.

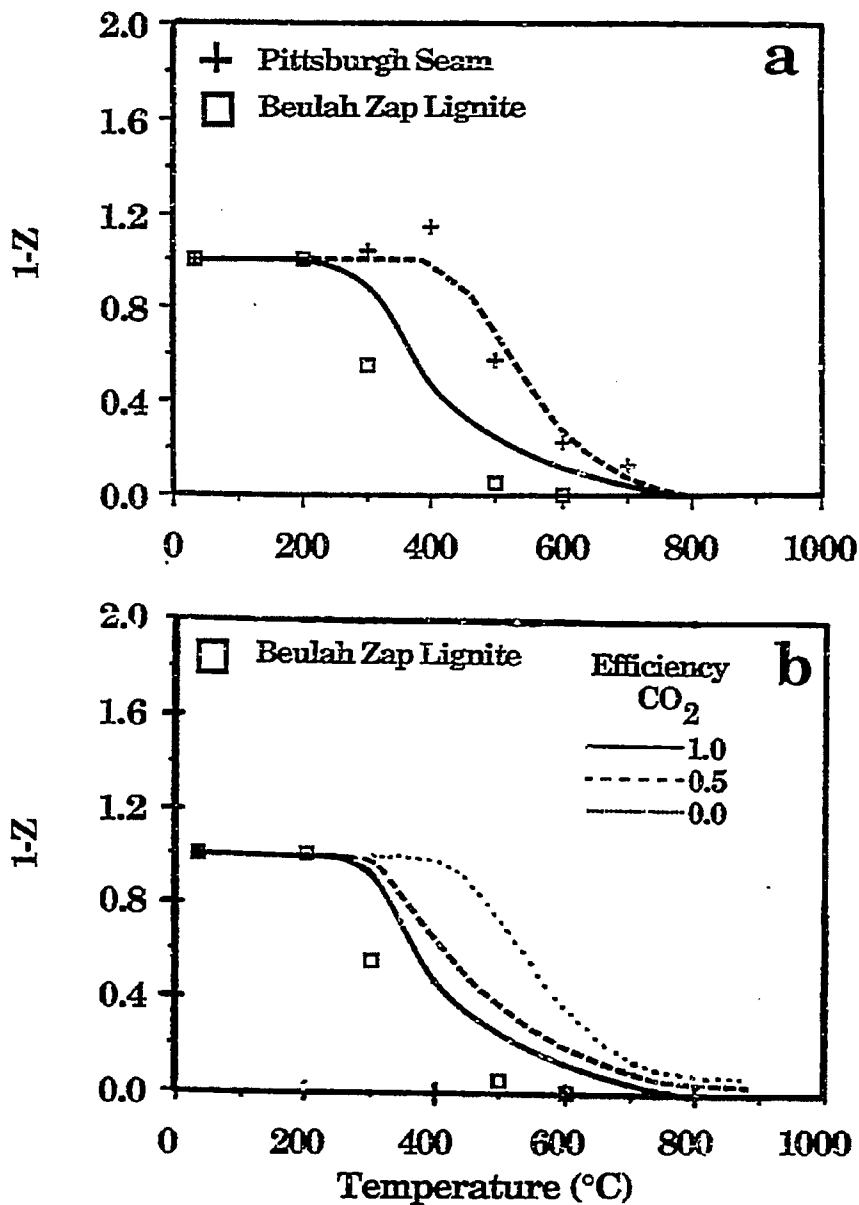


Figure 7. a) Comparison of Measured and Predicted Normalized Volumetric Swelling Ratio as a Function of Temperature. Solid Line is the Prediction of Beulah Lignite, Dashed Line is for Pittsburgh Seam Coal. The Crosslink Efficiency of CO₂ is 1.0. b) Effect of Crosslink Efficiency of CO₂ on the Normalized Volumetric Swelling Ratio Profile with Temperature. For a) and b) Heating Rate is 0.5°C/sec. ΔP = 0 atm.

The agreement between theory and experiment is good except that the increase in Z for the Pittsburgh Seam coal in Fig. 7a is not predicted. This may be related to the restrictions of assumption (n). The predictions in Fig. 2a are different from those originally presented in Ref. 50. In Ref. 50, the value used for VSR_{min} was not appropriate for the fully crosslinked molecule. This error has now been corrected.

In Fig. 7b, the effect of varying the CO_2 crosslinking efficiency is considered. The figure shows cases calculated for the lignite assuming 0, 0.5, and 1.0 crosslinks are formed per CO_2 evolved. Varying this assumption has a major effect on the early crosslinking of the lignite. Assuming that the crosslinking efficiency per CO_2 is 1.0 gives the best agreement with the data.

The difference in crosslinking behavior between the two coals is manifested in several areas. At low heating rates, the Pittsburgh Seam chars soften, the Beulah, Zap chars do not. This is in agreement with the high predicted maximum extract yields in the Pittsburgh char (70%) compared to the low extract yields in the Beulah, Zap lignite (7%). The measured values are 71% (Ref. 16) and ~6%, respectively. The predicted yield of tar plus aliphatic gases at 1 atmosphere, 0.5°C/sec to 900°C, of 26% is in good agreement with the measured value of 28% for the Pittsburgh Seam coal. The predicted value of 11% (for $\Delta P = 10$ atm) is in good agreement with the measured value of 10% for the Beulah, Zap lignite.

Molecular Weight Distribution. A sensitive test of the general model is the ability to predict the tar molecular weight distribution and its variations with rank, pressure and heating rate. The input to the model is the distribution of monomer molecular weights. The tar, which consists of oligomers, has a different distribution from the monomer distribution and is controlled by the relative

effects of bond breaking, crosslinking and transport. The tar molecular weight distribution is not highly sensitive to the choice of M_{avg} and σ . For Pittsburgh Seam coal, the average monomer was assumed to be a three ring compound ($M_{avg} = 256$) and a fairly broad distribution ($\sigma = 250$) was chosen. The same values appeared to work for the lignite. These are in reasonable agreement with the measured values of ~ 300 reported by Solum et al. (79) for both coals.

Figures 8c and 8d show results for the Pittsburgh Seam bituminous coal and the Beulah, Zap lignite pyrolyzed in the FIMS apparatus. The data have been summed over 50 amu intervals. While the Pittsburgh bituminous coal shows a peak intensity at about 400 amu, the lignite peak is at 100 amu. The predicted average tar molecular weight distributions are in good agreement with FIMS data as shown in Fig. 8a and 8b. Since both tar distributions are from the same monomer distribution, the enhanced drop off in amplitude with increased molecular weight for the lignite compared to the bituminous coal must be due to early crosslinking and transport effects in the lignite.

Pressure Effects. The predicted effect of pressure on the tar molecular weight distribution is illustrated in Figs. 9a and 9b. Pressure enters the model through the transport Eqs. 3 and 4. The internal transport rate (Eq. 4), which is assumed to dominate, is inversely proportional to the ambient pressure P_0 . The reduced transport rate reduces the evolution rate of the heavier molecules. Therefore, the average molecular weight and the vaporization "cut-off" decrease with increasing pressure. The trends are in agreement with observed tar molecular weight distributions shown in Figs. 9c and 9d. The spectra are for previously formed tar which has been collected and analyzed in a FIMS apparatus (60). The low values of intensity between 100 and 200 mass units are believed to be due to loss of these components due to their higher volatility.

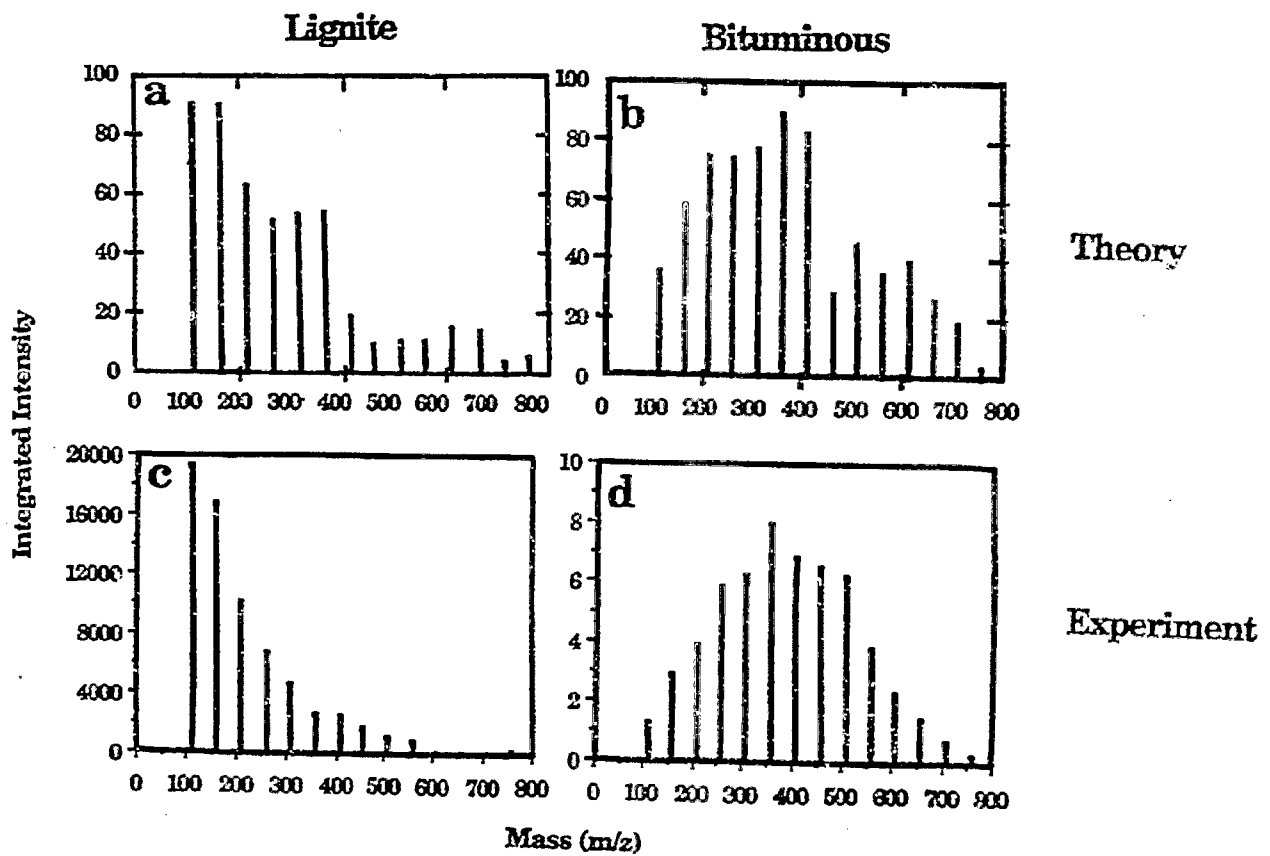


Figure 8. Comparison of Measured and Predicted Tar Molecular Weight Distributions for Lignite and Bituminous Coals. The Experiments are Performed by Pyrolysis of Coal Samples in a FIMS Apparatus. Intensities have been Summed Over 50 amu Intervals. $\Delta P = 0.0$ atm.

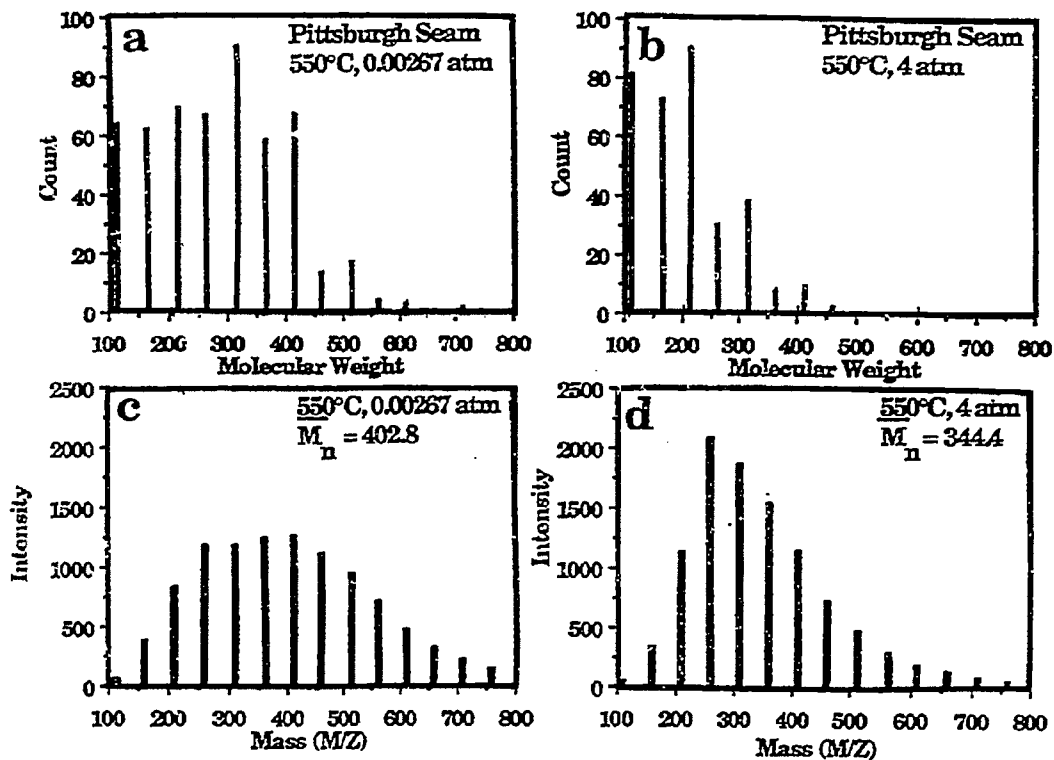


Figure 9. Comparison of Predicted (a and b) and Measured (c and d) Tar Molecular Weight Distribution for Pyrolysis of a Pittsburgh Seam Coal in a Heated Grid Apparatus at a Heating Rate of 500°C/sec to 550°C. Figure a and c Compare the Prediction and the Measurement at .00267 atm. Figure b and d Compare the Prediction and Measurement at 4.0 atm. $\Delta P = 0.2$ atm.

Pressure effects on yields have also been examined. Figure 10 compares the predicted and measured pressure dependence on yield for a Pittsburgh Seam coal. Figure 10a compares to the total volatile yield data of Anthony et al. (22) while Fig. 10b compares to the tar plus liquids data of Suuberg et al. (7). The agreement between theory and experiment is good at one atmosphere and above, but the theory with $\Delta P = 0$ (solid line) overpredicts the yields at low pressure. Below one atmosphere, it is expected that ΔP within the particle will become important compared to the ambient pressure, P_0 . The dashed lines, which agree with the data, were obtained assuming $\Delta P = 0.2$ atm, which is physically reasonable.

Heating Rate Effects. It is well known that heating rate can affect the amount of volatiles produced (29,76,84-86). Heating rate can also affect the melting and swelling behavior of low rank coals (13). Considering the mechanisms proposed for pyrolysis (including those in this paper), it is the relative rates of competing processes for tar formation (e.g., bond breaking, crosslinking, and mass transport) which provide the heating rate effects. The relative rates of these processes change with temperature and it is the heating rate which determines the temperature at which the controlling reactions occur. So it is really the temperature of tar formation not the heating rate per se which is important.

Consider first the effects of heating rate on the yields of a Pittsburgh Seam bituminous coal. Table III summarizes the results for three experiments (16,87,88) in which the heating rate varied from 0.5 to 5000°C/sec and in which the final temperature reached is sufficiently high for tar formation to be completed during the heating period. As can be seen, the predicted and measured volatile yields increased by about 10% from low to high heating rates. As can also be seen, the increase in yield results from the increase in tar plus aliphatic gases.

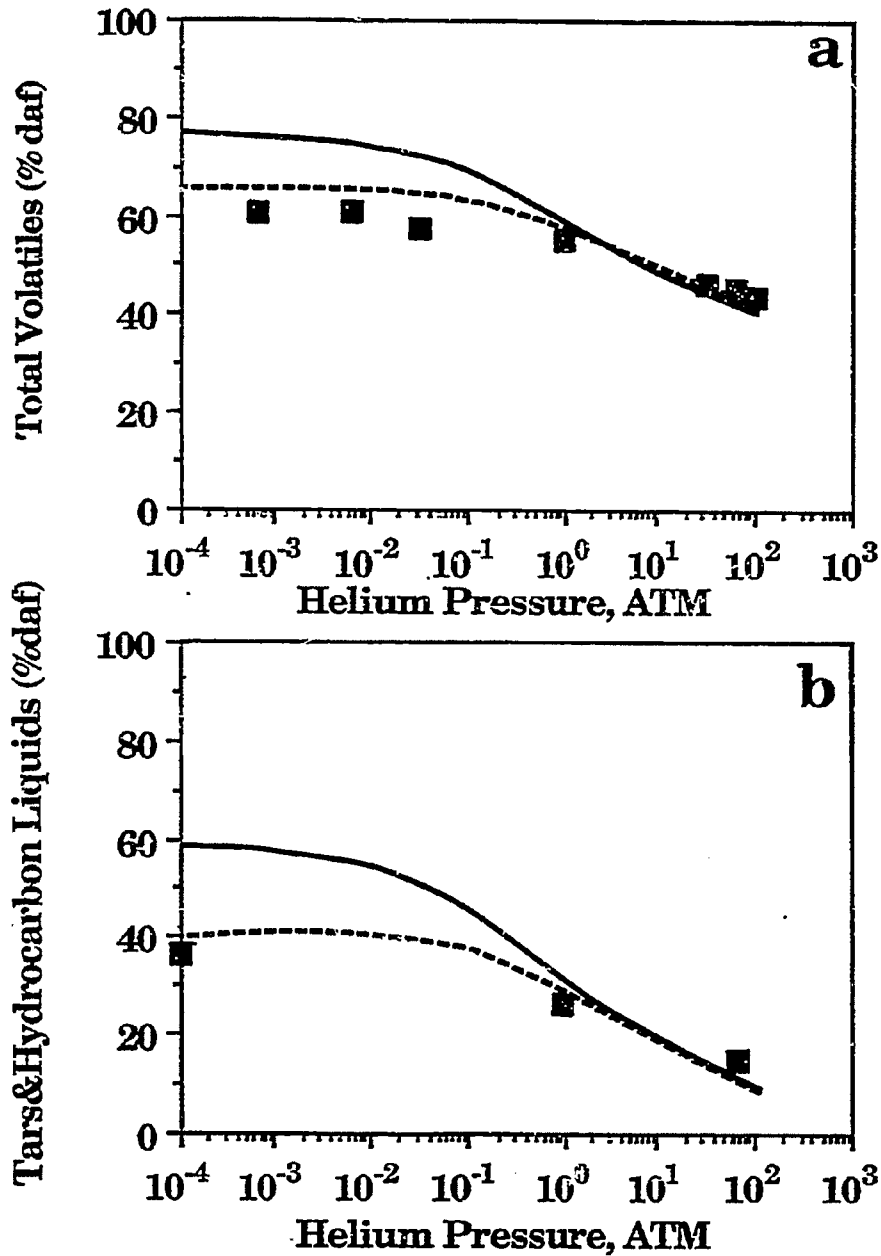


Figure 10. Comparison of Measured and Predicted Volatile Pressure for a Pittsburgh Seam Bituminous Coal. a) Total Volatiles; Data of Anthony et al. (22). b) Tars and Hydrocarbon Liquids; Data of Suuberg et al. (7). Solid Line Assumes $\Delta P = 0$ atm, Dashed Line Assumes $\Delta P = 0.2$ atm

Table III - Comparison of Measured and Predicted Yields for Pittsburgh Seam Bituminous Coal.
 ($\Delta P = 0$ atm)

Experiment	Heating Rate °C/s	P_0 ATM	Final Temperature	Maximum Yield		Total Maximum	
				Tar + Aliphatic Gases		Volatiles (wt.%)	
				Measured	Predicted	Measured	Predicted
TG-FTIR	0.5	1.0	600°C	25	29	35	37
Entrained Flow	5000	1.0	700°C	36	37	43	43
Heated Grid	640	.85	745°C	---	40	47	47

Examination of the rates in the model shows that the major contribution to the variation in yield is the internal transport rate relative to the bond breaking rate. At low temperatures, internal transport severely limits the evolution of the heavier molecules resulting in smaller tar molecules and inefficient use of the donatable hydrogens.

A set of data showing the effect of heating rate on yield for the Argonne Pittsburgh Seam coal was recently reported by Gibbins-Matham and Kandiyoti (84). Data were obtained in a wire grid apparatus at 1°C/sec and 1000°C/sec with no holding time and at 1000°C/sec with a 30 sec hold. These data (triangles) are compared to predictions of the model in Fig. 11. For all three cases, the theory predicts the correct pyrolysis final yields, the correct yield variation with heating rate and the correct temperature shift with heating rate.

The predicted yields, however, occur at temperatures from 20-80°C higher than the comparable experimental yields. At this time, the reason for the discrepancy is not clear. One possible reason is the assumptions used for the internal transport limitations. Calculations were made assuming that molecules for which $P_j \geq P_0 + \Delta P$ evolve as they are produced, while only heavier molecules evolve as described in Eq. 4. The predicted curves (dashed lines in Fig. 11) are 20-40°C lower than in the original calculation. Alternatively, the vapor pressure may not be accurately described by the expression of Suuberg et al. (32). Oh (89) compared a number of correlations for the tar vapor pressure. At 1000°C, the expression of Suuberg et al. (32) gave vapor pressures from one to two orders of magnitude lower than other published expression (90,91). Calculations using the expression for aliphatic molecules of Maiorella (90) gave predictions at about 40°C lower temperatures, in better agreement with data of Gibbins-Matham and Kandiyoti. The simulation, however, required a lower value of W_B (0.060) to compensate for the

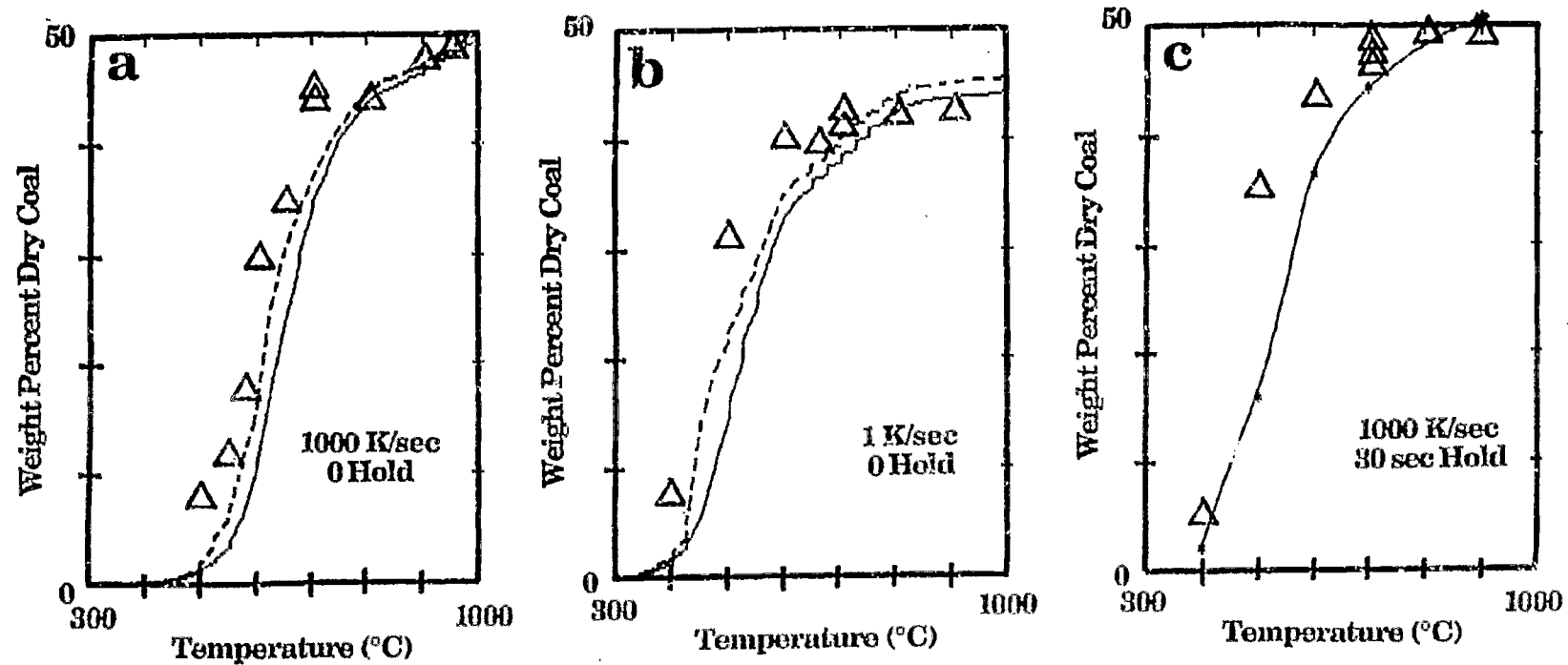


Figure II. Comparison of FG-DVC Model Predictions with the Data of Gibbins-Matham and Kandiyoti (83) (symbols) for Pittsburgh Seam Coal. a) 1000 K/s, Zero Hold, b) 1 K/s, Zero Hold, and c) 1000 K/s, 30 s Hold. $P = 1.18$ atm. Transport by Eq. 4 ($\Delta P = 0$) and no External Transport Limitation. The Dashed Line Assumes no Transport Limitations for Molecules whose Vapor Pressure Exceeds $P_0 + \Delta P$.

higher volatility. Predictions using the same assumptions failed to match those of Fong et al. (16) in Fig. 6 with regard to the temperature of evolution and the amount of extract produced. Possible refinements of the internal transport model are being considered.

Another possible explanation for the discrepancy is the accuracy of the reported pyrolysis temperature which has been notoriously variable among investigators. Other Pittsburgh Seam coal data (not shown) from Niksa et al. (40) under the same conditions as Fig. 11c (1000°C/sec, 30° sec hold) and from Oh (89) and Suuberg et al. (7) for the same conditions as Fig. 11a (1000°C/sec, zero hold) show substantial variations in temperature compared to the results of Gibbons-Matham and Kandiyoti (84). The theoretical predictions would lie within the scatter of the several data sets. Work is in progress to resolve this question.

Low rank coals also exhibit heating rates effects. It has been found that Beulah lignite chars soften and exhibit bubble formation at high heating rates (~20,000°C/s) (13). Under these conditions, molecular weight distribution of tars of Beulah lignite look like that of a bituminous coal (30,31). The infrared spectrum of the tar is also closer in appearance to that of the parent coal (31). The mass spectra of the tars formed at high heating rate (20,000°C/s) and low heating rate (0.05°C/s) are shown in Figs. 12a and 12b, respectively. The low values of intensity between 100 and 200 mass units in Fig. 12b are believed to be due to loss of these components due to their high volatility. The molecular weight distribution of the tars is very sensitive to the heating rate. The effect is attributed to the higher rate of depolymerization reactions relative to crosslinking reactions at high temperatures, as discussed in the sensitivity section.

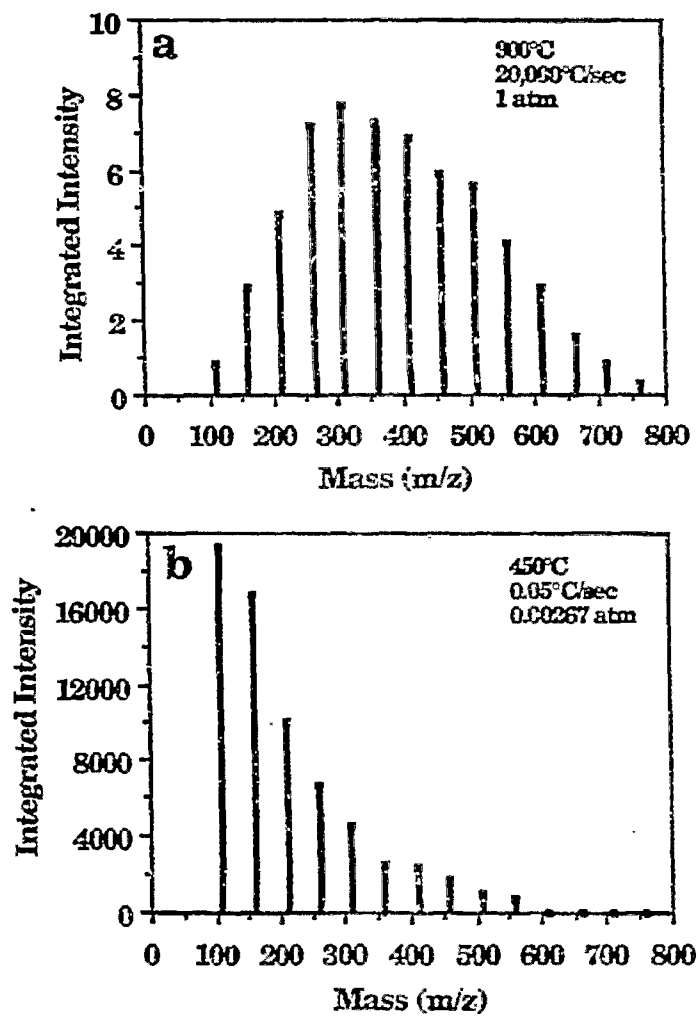


Figure 12. Comparison of FIMS Spectra of Tars of Beulah Zap Lignite Formed at a) High Heating Rate (20,000°C/sec) and b) Low Heating Rate (0.05°C/sec).

The FG-DVC model, assuming the internal mass transport limitations, was used to simulate the low heating rate (0.05°C/s) and high heating rate (20,000°C/s) pyrolysis of Beulah lignite. The activation energy for CO₂ (extra loose) in the FG subroutine was reduced from 60 kcal/mole to 45 kcal/mole in order to make it lower than the activation energy for bond breaking (55 kcal/mole). This was done since measurements of the rate of crosslinking at high heating rates suggested that the relative rate of bond breaking and crosslinking reactions associated with CO₂ evolution is increased with increasing temperature (92). This change in the activation energy makes only a slight change in the CO₂ evolution profiles for high heating rate (20,000°C/s) and low heating (0.5°C/s) predictions. The CO₂ gas evolution profiles are compared to the data in Figs. 13a and 13b for high heating rate (20,000°C/s) and low heating rate (0.5°C/s) experiments with Beulah lignite using activation energies of 60, 45 and 30 kcal/mole. When the activation energy for CO₂ (extra loose) evolution was reduced to 45 kcal/mole, acceptable fits to the gas evolution data were still obtained. However, at 30 kcal/mole, the high heating rate CO₂ evolution profile was quite different and did not agree with the experimental data.

The model, with internal mass transport limitations included, was used to simulate the tar molecular weight distributions with $\Delta P = 0$ atm for Beulah lignite for high heating rate (20,000°C/s) in Figs. 14a and 14b. The simulations were done for both the original activation energy (60 kcal/mole) and altered activation energy (45 kcal/mole) for CO₂ (extra loose) evolution. The tar molecular weight distributions (for $\Delta P = 0$ atm) at high heating rates (Figs. 14a and 14b) show the observed high values of the tar molecular weight at heating rate (Fig. 12a). The lower activation energy case (Fig. 14a) exhibits more high molecular weight molecules and gives a higher tar yield (10%) than the high activation energy case (8%) (Fig. 14b). The low heating rate (0.05°C/s) case ($\Delta P = 0$) (Fig. 14c),

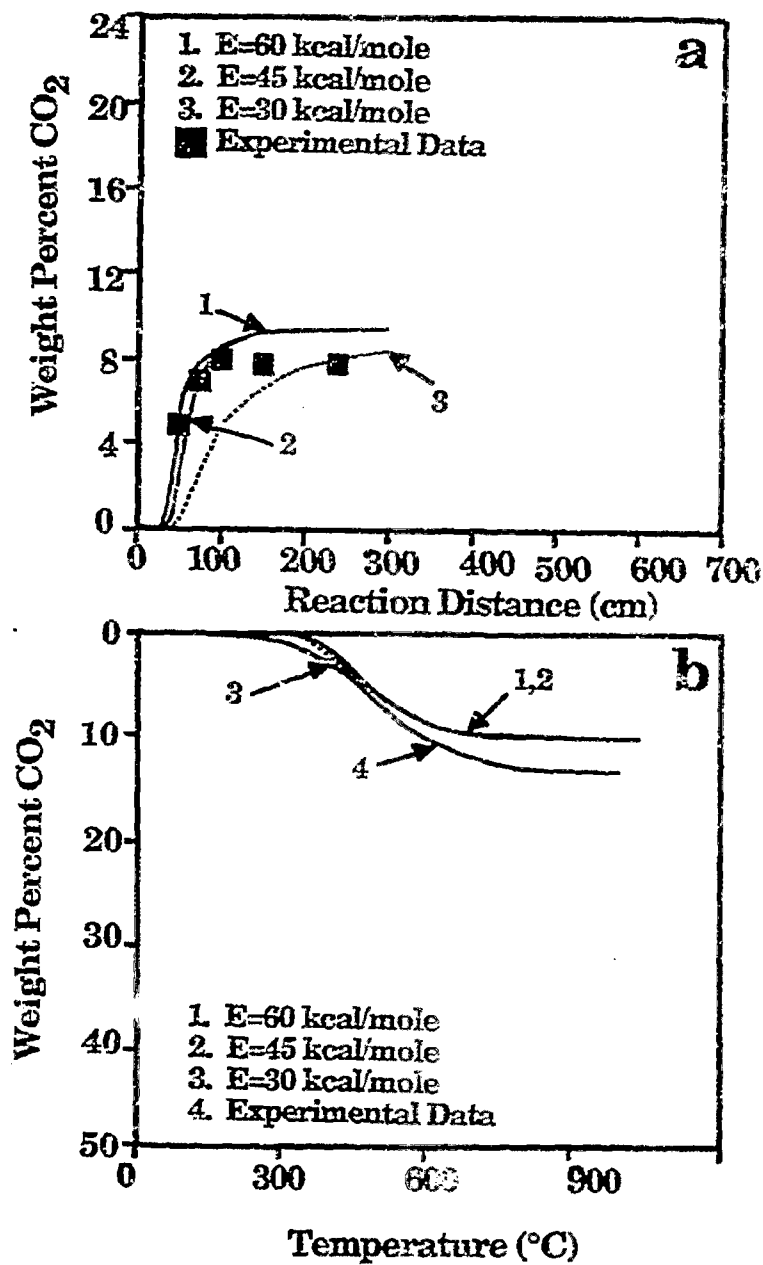


Figure 13. Comparison of CO₂ Evolution Data from North Dakota Lignite for Low Heating Rate (0.5°C/sec) and High Heating Rate (20,000°C/sec) Experiments with Model Predictions for Different Values of Activation Energy for CO₂ (extra loose) in the FG-DVC Model. a) Heated Tube Reactor Experiments (6) and b) TG-FTIR Experiments (6).

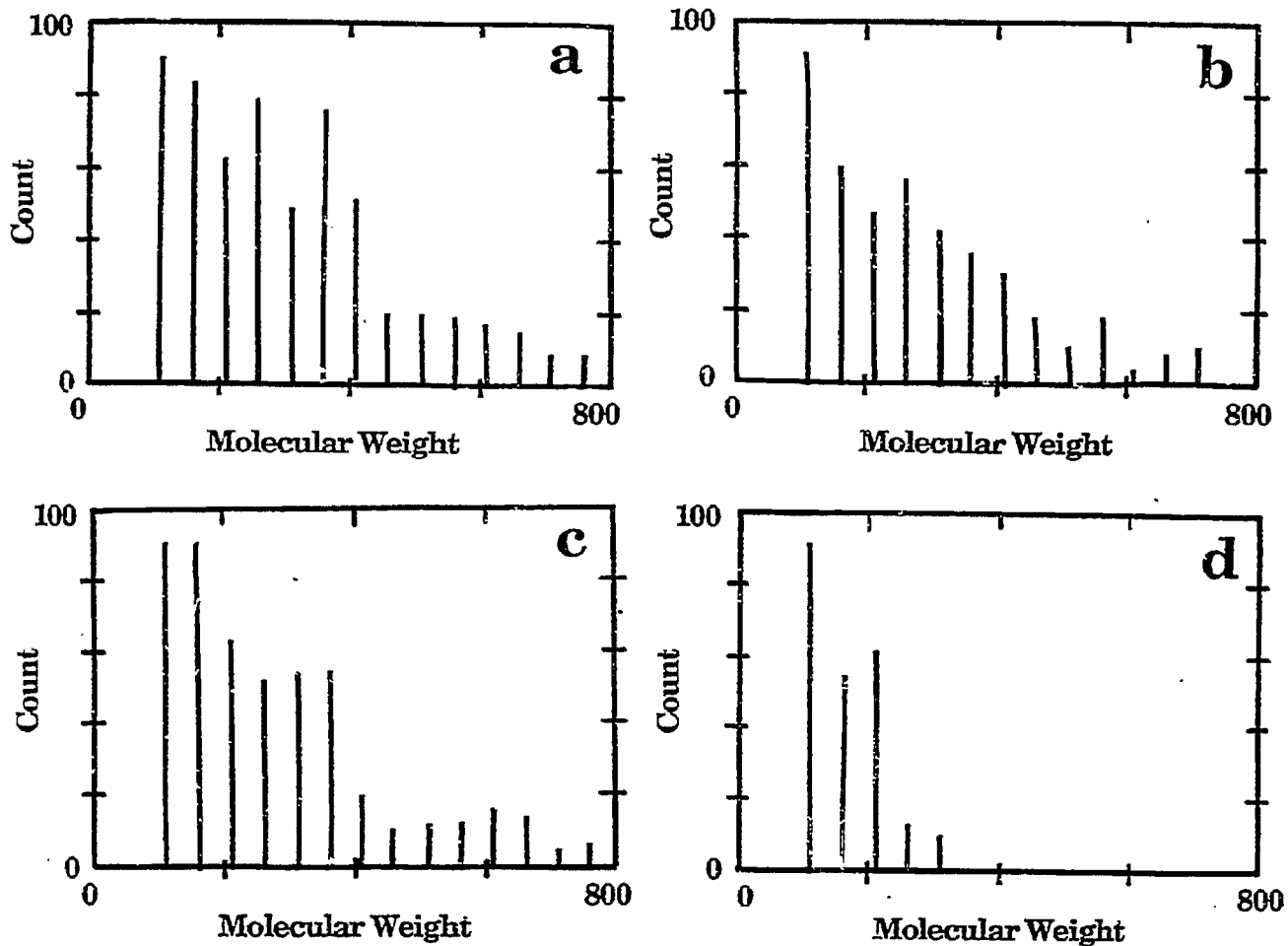


Figure 14. Comparison of Predicted Molecular Weight Distribution of Tars of Beulah Lignite for a) and b) High Heating Rate (20,000°C/sec), c) and d) Low Heating Rate (0.05°C/sec). In a), c) and d) the CO₂ Activation Energy is 45 kcal/mole and in b) it is 60 kcal/mole. In a), b), and c) $\Delta P = 0$ atm and in d) $\Delta P = 10$ atm.

exhibits lower molecular weights consistent with Fig. 12b. At high heating rates, where crosslinking reactions are curbed and the lignite melts, ΔP is likely to be low. At low heating rate, due to the higher extent of crosslinking before tar evolution, the coal is less fluid and hence, ΔP (which is related to viscosity of the solid/liquid mixture) is likely to be higher. A simulation for the slow heating rate case with $\Delta P = 10$ atm is shown in Fig. 14d. The measured molecular weight distribution in Fig. 12b appears to be intermediate between the $\Delta P = 0$ and $\Delta P = 10$ atm cases.

Sensitivity Analysis. This section considers the sensitivity of the FG-DVC model to variations in the DVC parameters. The FG parameter sensitivities have been considered elsewhere (52).

a) **Variations in W_B .** The number of labile bridges is the most important parameter in determining tar yield. The value of W_B for the Pittsburgh Seam coal was reduced from its value of 9.4 to 7.4 and 5.4. The results in Fig. 15a were calculated for the case considered in Fig. 6d. The reduction in W_B reduces the tar yield, the total volatile yield and the extract yield. Higher values of W_B could not be considered because the molecule already contained the maximum number of labile bridges. This is a limitation in the model as it is currently formulated since all the donatable hydrogens are assumed to be in bridges.

b) **Variations in L .** The parameter L affects mainly the extract yield in the raw coal. Figure 15b demonstrates variations in L from 6 to 10 around the base value of 7. The initial extract yield varies substantially while there is only a minor effect on the tar yield, total volatile yield, and extract yield at elevated temperature.

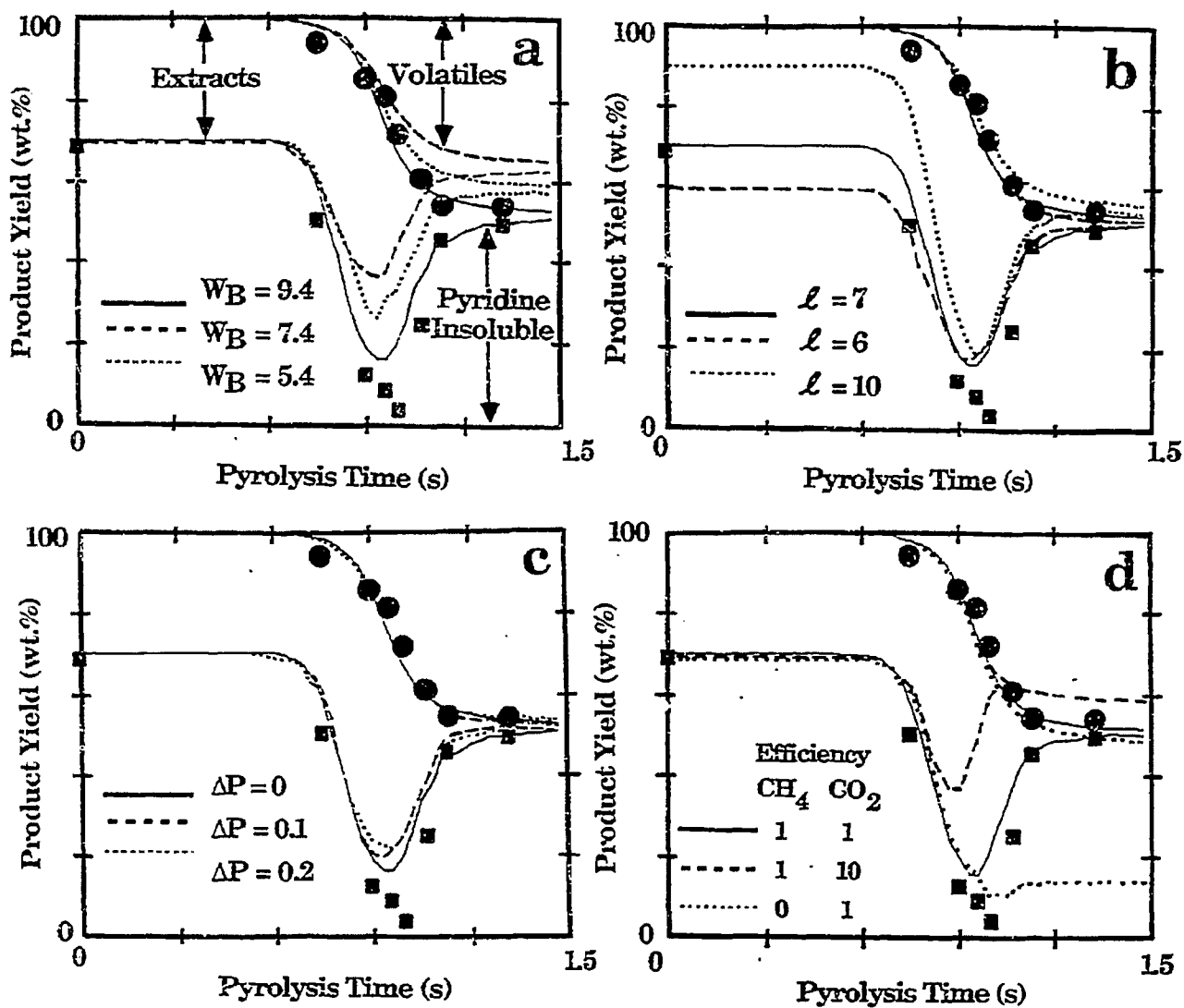


Figure 15. Effect on Product Yields of: a) Fraction of Labile Bridges, W_B , b) Oligomer Length, ℓ , c) Internal Pressure Difference ΔP , and d) Crosslinking Efficiency. Data is of Fong et al. (16) for Pittsburgh Seam Bituminous Coal (1018K @ 640 K/s, $P = 0.85$ atm) $\Delta P = 0$ atm.

c) Variations in ΔP . The effect of variations in ΔP on the overall yield are considered in Fig. 10. There is no effect at one atmosphere pressure and above but a strong effect at lower ambient pressures. Figure 15c confirms that ΔP has little effect on the tar yield or the total volatile yield for pyrolysis at one atmosphere pressure. Only the extract yield is slightly affected.

Figure 16 illustrates the effect on the molecular weight distribution for three values of ΔP for pyrolysis in vacuum ($P_0 = 0$). The yield of higher molecular weight tars present for $\Delta P = 0$ is lower for $\Delta P = 0.1$ atm, and eliminated for $\Delta P = 0.2$ atm. The total tar yields are 39%, 21% and 17% for $\Delta P = 0, 0.1$ and 0.2 atm respectively. The tar molecular weight distribution for $\Delta P = 0$ atm gives the best match to Fig. 9c, but $\Delta P = 0.1$ to 0.2 atm provides the best match to the yield.

The variation of ΔP in the tar molecular weight distribution for lignite is discussed with reference to Fig. 13.

d) Variations in $m(\text{CO}_2)$ and $m(\text{CH}_4)$. Variations in $m(\text{CO}_2)$ were considered for the lignite in the discussion accompanying Fig. 7. Variations in both $m(\text{CO}_2)$ and $m(\text{CH}_4)$ are considered in Fig. 15d. These have a major effect on the yields. Increasing $m(\text{CO}_2)$ from 1 to 10 reduces the extract and volatile yields while reducing $m(\text{CH}_4)$ from 1 to 0 prevents the repolymerization of the extract.

e) Variations in M_c . Variations in the M_c values were made. These chiefly affect the extract yield, requiring an adjustment in \mathcal{L} . They have little effect on the subsequent crosslinking in the coal. The reason for this can be seen in Table I. The initial value of M_c consistent with the literature required only 0.09 and 0.18 crosslinks/monomer for the bituminous coal and lignite, respectively. The

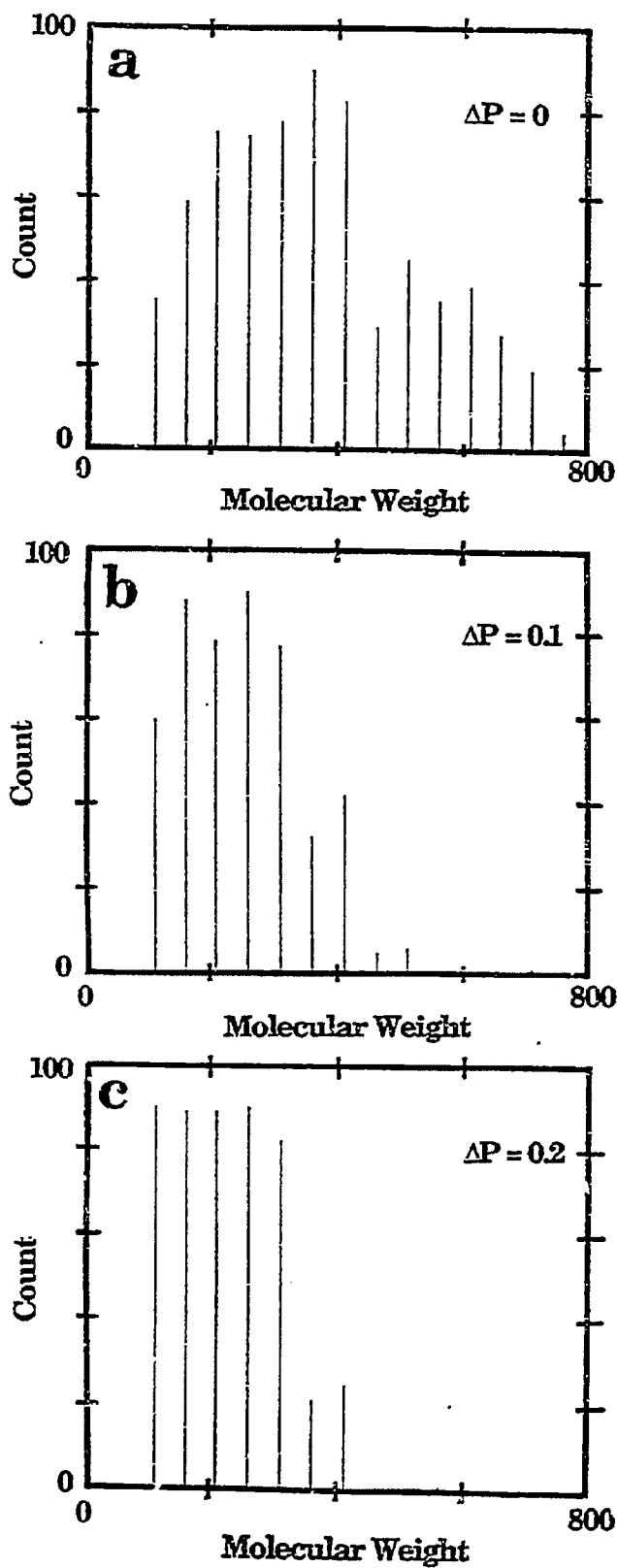


Figure 16. Effect of ΔP on Tar Molecular Weight Distribution for Pittsburgh Seam Bituminous Coal Heated to 723K @ 0.05 K/s, $P = 0.00267$.

total crosslinks added during pyrolysis are .49 and .89, respectively. The added crosslinks is thus much larger than that in the raw coal, and, consequently, dominates the char's behavior.

f) Variations in M_{avg} and σ . Figures 17a, b, and c illustrate the effects of variations in M_{avg} . Varying M_{avg} changes the shape of the tar spectrum, but not drastically. The shape is still dominated by the transport properties (e.g., see Fig. 16). The effect on the tar yield is also modest, giving values of 46%, 44%, and 42% for M_{avg} values of 156, 256, and 356, respectively.

A similar lack of sensitivity of the molecular weight distribution to M_{avg} was exhibited for the lignite for both high heating rate ($\sim 20,000^\circ\text{C}/\text{sec}$) and low heating rate ($0.05^\circ\text{C}/\text{sec}$) cases (not shown).

The effect of variations in σ is illustrated in Figs. 17d, e and f. $\sigma = 250$ fills in the spectrum in a more realistic fashion and is more aesthetically pleasing than the two smaller values of σ . The effect on the total tar yield is minor with yields of 41%, 46%, and 45% for $\sigma = 0, 50, \text{ and } 250$, respectively.

g) Variations in W_N . This parameter which is taken from the FG model controls the split between tar, char, and gas.

h) Vaporization Law. The results are sensitive to the choice of the tar vapor pressure correlation. Higher vapor pressures result in faster tar evolution and higher yields as discussed in reference to Fig. 11.

A summary of the sensitivity analysis is presented in Table IV. The concentration of labile bridges W_3 and the CO_2 crosslinking parameter $m(\text{CO}_2)$ are

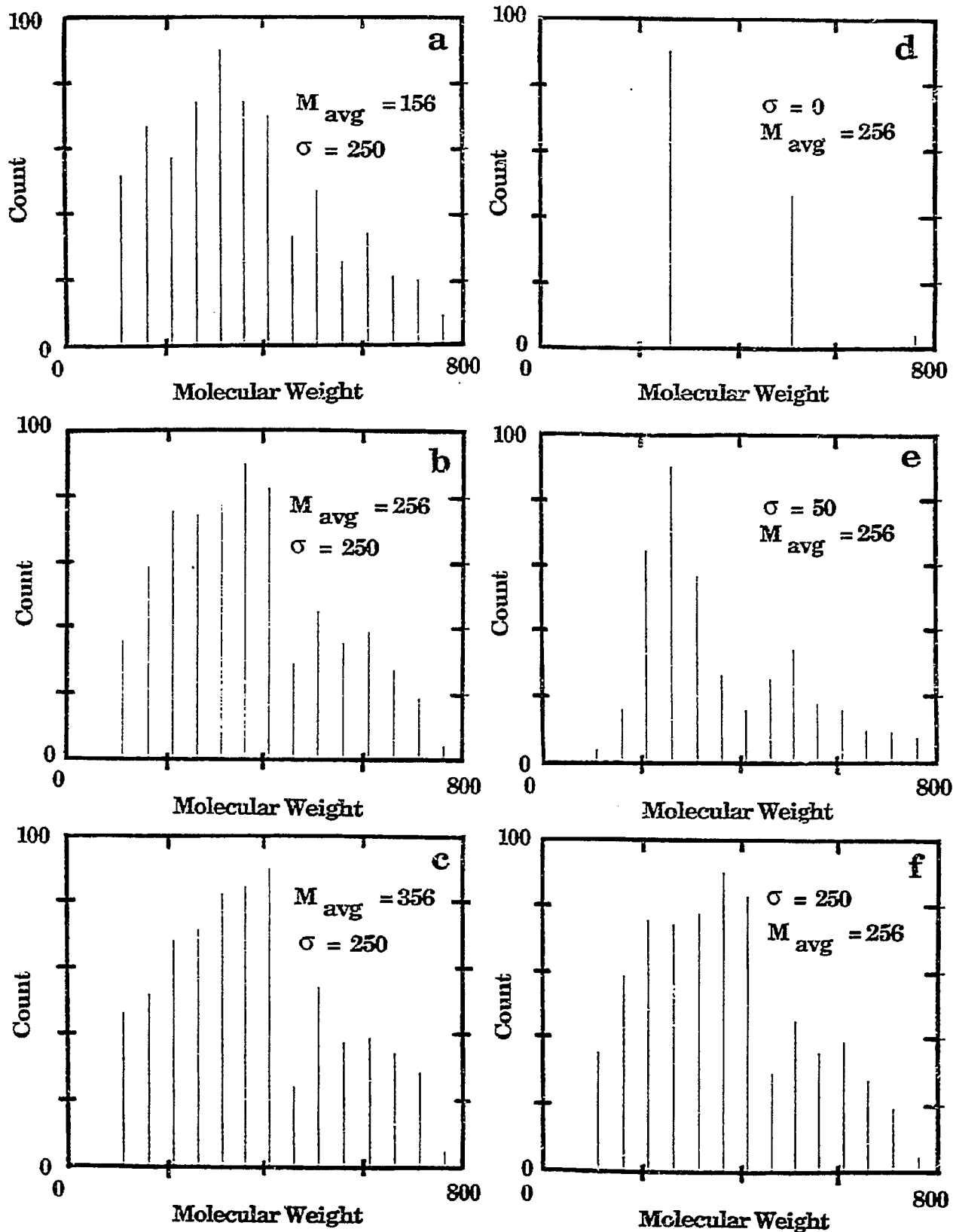


Figure 17. a-c) Effect of M_{avg} on the Shape of the Tar Spectrum and d-f) Effect of σ on the Shape of the Tar Spectrum. Heating Rate is $0.05^\circ\text{C}/\text{sec}$ to 450°C , $P = 0.00267$ atm and $\Delta P = 0$ atm.

TABLE IV

SUMMARY OF SENSITIVITY ANALYSIS

	W_N	W_B	\mathcal{L}	M_C	$m(\text{CO}_2)$	$m(\text{CH}_4)$	M_{avg}	α	ΔP
Tar Molecular Weight	W	W	W	W	S	W	M	M	S
Tar Yield	S	S	W	W	S	M	W	W	S
Char Extract Yield	W	S	W	W	S	S	W	W	M
Coal Extract Yield	W	W	S	M	W	W	W	W	W
Char Solvent Swelling Ratio	W	W	W	S	S	S	W	W	W
Coal Solvent Swelling Ratio	W	W	W	W	W	W	W	W	W

W = Weak or none

M = Moderate

S = Strong

most important parameters in determining yields.

CONCLUSIONS

A general FG-DVC model for coal devolatilization which combines a functional group model for gas evolution and a statistical model for tar formation has been presented. The tar formation model includes depolymerization, crosslinking, external transport and internal transport. The crosslinking is related to the evolutions of CO₂ and CH₄, with one crosslink formed per molecule evolved. The predictions of the tar formation model are made using Monte Carlo calculation methods. Predictions take between 10 sec and 10 min, (depending on coal rank, experimental conditions and accuracy required) on a Sun 3/260 computer.

The FG-DVC model predictions compare favorably with a variety of data for the devolatilization of Pittsburgh Seam coal and North Dakota (Beulah) lignite, including volatile yields, extract yields, crosslink densities and tar molecular weight distributions. The variations with pressure, devolatilization temperature, rank and heating rate were accurately predicted. Comparison of the model with several sets of data employing alternative assumptions on transport suggests assuming that the particle is well mixed (i.e. the surface concentration of tar molecules is the same as the bulk) overpredicts the transport rate. For 50 μm particles, assuming that the internal transport limitation dominates (i.e. neglecting the external transport) provides a good fit to the data. This is consistent with: a) assuming that the internal and external transport mechanisms act in series, or b) they act in parallel but liquid phase diffusion of tar molecules to the surface is very small and so the external transport term can be neglected.

The rank dependence of tar formation, extract yields, crosslinking, and viscosity appears to be explained by the rank dependence of CO₂ yields. The high CO₂ yields in low rank coals produce rapid crosslinking at low temperatures and hence low tar yields, low extract yields, loss of solvent swelling properties and high viscosities. The relative importance of crosslinking compared to bond breaking is, however, sensitive to heating rate and this effect is predicted by the FG-DVC model. The predicted crosslinking associated with methane evolution appears to match the observed crosslinking in high rank coals (which evolve little CO₂).

The model has eight coal structure parameters which must be determined for each coal from selected laboratory experiments. Once determined, these remain fixed for all experiments. The model also contains one adjustable parameter, ΔP , the internal pressure difference which drives the volatiles out of the particle. A sensitivity analysis shows that the volatile yield is most sensitive to the fraction of labile bridges, W_B , the crosslinking efficiency parameters $m(\text{CO}_2)$ and $m(\text{CH}_4)$, and, in some cases (low rank coals, low pressure), to ΔP . The monomer molecular weight distribution parameters, M_{avg} and σ , have only a weak effect on yields and tar molecular weight distributions. The initial molecular weight between crosslinks, M_c , and the initial oligomer length, \mathcal{L} , affect the coal's solvent swelling ratio and extract yield but have little effect on the subsequent pyrolysis behavior.

The model currently has several deficiencies. There is no model for estimating liquid phase diffusion of tar molecules which may be important for very small particles. The calculation of the average molecular weight between crosslinks neglects the effect of labile bridge rupture. The assumption that all the donatable hydrogen is in bridges may be restrictive for some high hydrogen

coals. The model presented here has neglected polymethylenes in coal and the effect of other types of weak bonds besides ethylene bridges. There are some discrepancies between the predictions and reported temperatures of pyrolysis experiments. It is unclear at this time whether this is due to errors in the reported temperatures or in the transport predictions. Many of these deficiencies require only minor modifications to the model and are currently being addressed.

ACKNOWLEDGMENT

This work was supported under DOE Contracts DE-AC21-85MC22050, DE-AC21-84MC21004, DE-AC21-86MC23075 and DE-FG22-85PC80910. The authors wish to express their thanks to Professor Eric Suuberg for many helpful discussions on transport properties, and to Dr. Zhen Zhong Yu for assistance with the model calculations.

REFERENCES

1. Howard, J.B., Peters, W.A., and Serio, M.A., "Coal Devolatilization Information for Reactor Modeling", Final Report EPRI Project No. 985-5, (1981).
2. Howard, J.B., Chemistry of Coal Utilization, (M.A. Elliott, Ed.), John Wiley, NY, Chapter 12, p 665, (1981).
3. Gavalas, G.R., Coal Pyrolysis, Elsevier Sci., Amsterdam, The Netherlands, (1982).
4. Suuberg, E.M., in Chemistry of Coal Conversion, (R.H. Schlosberg, Ed.), Chapter 4, Plenum Press, NY (1985).
5. Solomon, P.R. and Hamblen, D.G., in Chemistry of Coal Conversion, (R.H. Schlosberg, Editor), Plenum Press, NY, Chapter 5, pg. 121, (1985).
6. Serio, M.A., Hamblen, D.G., Markham, J.R., and Solomon, P.R., Energy and Fuels, 1, (2), 138, (1987).
7. Suuberg, E.M., Peters, W.A., and Howard, J.B., 17th Symp. (Int) on Combustion, The Combustion Institute, Pittsburgh, PA, pg. 117, (1979).
8. Juntgen, H. and van Heek, K.H., Fuel Processing Technology, 2, 261, (1979).
9. Weimer, R.F. and Ngan, D.Y., ACS Div. of Fuel Chem. Preprints, 24, #3, 129, (1979).
10. Campbell, J.H., Fuel, 57, 217, (1978).
11. Solomon, P.R. and Colket, M.B., 17th Symposium (Int) on Combustion, The Combustion Institute, Pittsburgh, PA, 131, (1979).
12. Solomon, P.R., Hamblen, D.G., Carangelo, R.M., and Krause, J.L., 19th Symposium (Int) on Combustion, The Combustion Institute, Pittsburgh, PA, 1139, (1982).
13. Solomon, P.R., Serio, M.A., Carangelo, R.M., and Markham, J.R., Fuel, 65, 182, (1986).
14. Xu, W.-C., and Tomita, A., Fuel, 66, 627, (1987).
15. Juntgen, H., Fuel, 63, 731, (1984).
16. Fong, W.S., Peters, W.A., and Howard, J.B., Fuel, 65, 251, (1986).
17. Oh, M., Peters, W.A., and Howard, J.B., Proc. of the 1983 Int. Conf. on Coal Sci., p 483, International Energy Agency, (1983).
18. Fong, W.S., Khalil, Y.F., Peters, W.A. and Howard, J.B., Fuel, 65, 195 (1986).
19. van Krevelen, D.W., Properties of Polymers, Elsevier, Amsterdam (1976).
20. Solomon, P.R., New Approaches in Coal Chemistry, ACS Symposium Series 169, American Chemical Society, Washington, DC, pp 61-71, (1981).
21. van Krevelen, D.W. and Schuyer, J., Coal Science, Elsevier, Amsterdam, (1957).
22. Anthony, D.B., Howard, J.B., Hottel, H.C., and Meissner, H.P., 15th Symp. (Int) on Combustion, The Combustion Institute, Pittsburgh, PA, pg. 1303, (1974).
23. Unger, P.E. and Suuberg, E.M., 18th Symp. (Int) on Combustion, The Combustion Institute, Pittsburgh, PA, pg. 1203, (1981).
24. Russel, W.B., Saville, D.A., and Greene, M.I., AIChE J., 25, 65, (1979).
25. James, R.K. and Mills, A.F., Letters in Heat and Mass Transfer, 3, 1, (1976).
26. Lawellen, P.C., S.M. Thesis, Department of Chemical Engineering, MIT, (1975).
27. Chen, L.W. and Wen, C.Y., ACS Div. of Fuel Chem. Preprints, 24, (3), p141, (1979).
28. Niksa, S. and Kerstein, A.R., Combustion and Flame, 66, (2), 95, (1986).
29. Niksa, S. Combustion and Flame, 66, #2, 111, (1986).
30. Solomon, P.R., Squire, K.R., Carangelo, R.M., proceedings of the International Conference on Coal Science, Sydney, Australia, pg. 945, (1985).
31. Solomon, P.R. and Squire, K.R., ACS Div. of Fuel Chem. Preprints, 30, #4, 347, (1985).

32. Suuberg, E.M., Unger, P.E., and Lilly, W.D., *Fuel*, **64**, 956, (1985).
33. Solomon, P.R., Hamblen, D.G., Carangelo, R.M., Serio, M.A., and Deshpande, G.V., *ACS Div. of Fuel Chem. Preprints*, **32**, #3, 83, (1987).
34. Gavalas, G.R. and Wilks, K.A., *AIChE*, **26**, 201, (1980).
35. Simons, G.A., *Prog. Energy Combust. Sci.*, **9**, 259, (1983).
36. Suuberg, E.M. and Sezen, Y., *Proc. of the 1985 Int. Conf. on Coal Sci.*, p 913, Pergamon Press, (1985).
37. Melia, P.F. and Bowman, C.T., *Combust. Sci. Technol.* **31**, 195 (1983); also An analytical model for coal particle pyrolysis and swelling, paper presented at the Western States Section of the Combustion Institute, Salt Lake City, 1982.
38. Oh, M.S., Peters, W.A., and Howard, J.B., 1983 Int. Conf. Coal Sci. Proceedings, 483, Aug. 15-19, Pittsburgh, PA (1983).
39. Kobayashi, H., Howard, J.B., and Sarofim, A.F., 16th Symposium (Int) on Combustion, The Combustion Institute, Pittsburgh, PA, pg. 411, (1977). and Kobayashi, H., Ph.D. Thesis, MIT Dept. of Mechanical Eng., Cambridge, MA, (1976).
40. Niksa, S., Heyd L.E., Russel, W.B., and Saville, D.A., 20th Symposium (Int) on Combustion, The Combustion Institute, Pittsburgh, PA, pg 1445, (1984).
41. Badzioch, S. and Hawksley, P.G.W., *Ind. Eng. Chem. Proc. Des. Dev.*, **9**, 521, (1970).
42. Maloney, D.J. and Jenkins, R.G., 20th Symposium (Int) on Combustion, The Combustion Institute, Pittsburgh, PA, pg. 1435, (1984).
43. Witte, A.B. and Gat, N., "Effect of Rapid Heating on Coal Nitrogen and Sulfur Release", presented at the DOE Direct Utilization AR&TD Contractor's Meeting, Pittsburgh, PA, (1983).
44. Solomon, P.R. and King, H.H., *Fuel*, **63**, 1302, (1984).
45. Solomon, P.R., Squire, K.R., and Carangelo, R.M., *ACS Div. of Fuel Chem. Preprints*, **29**, (1), 10, (1984).
46. Squire, K.R., Solomon, P.R., Carangelo, R.M., and DiTaranto, M.B., *Fuel*, **65**, 833, (1986).
47. Squire, K.R., Solomon, P.R., DiTaranto, M.B., and Carangelo, R.M., *ACS Div. of Fuel Chem. Preprints*, **30**, #1, 386, (1985).
48. Gavalas, G.R., Cheong, P.H., and Jain, R., *Ind. Eng. Chem. Fundam.* **20**, 113, (1981).
49. Gavalas, G.R., Cheong, P.H., and Jain, R., *Ind. Eng. Chem. Fundam.* **20**, 122, (1981).
50. Solomon, P.R., Hamblen, D.G., Carangelo, R.M., Serio, M.A., and Deshpande, G.V., *Combustion and Flame*, **71**, 137, (1988).
51. Solomon, P.R., Hamblen, D.G., Deshpande, G.V. and Serio, M.A., *Coal Science and Technology 11*, (J.A. Moulijn, K.A. Nater, and H.A.G. Chermin, Eds.), pg. 601, Elsevier Science Publishers, Amsterdam, (1987).
52. Solomon, P.R. and Hamblen, D.G., *Prog. Energy Combust. Sci.*, **9**, 323, (1983).
53. Xu, W.C. and Tomita, A., *Fuel*, **66**, 632, (1987).
54. Agarwal, P.K., *Fuel*, **64**, 870, (1985).
55. Agarwal, P.K., Agnew, J.B., Ravindran, N. and Weimann, R., *Fuel*, **66**, 1097, (1987).
56. Vorres, K.S., *ACS Div. of Fuel Chem. Preprints*, **32**, (4), 221, (1987).
57. Green, T.K., Kovac, J., and Larsen, J.W., *Fuel*, **63**, #7, 935, (1984).
58. Green, T.K., Kovac, J., and Larsen, J.W., in *Coal Structure*, (R.A. Meyers, Editor), Academic Press, NY, (1982).
59. Suuberg, E.M., Lee, D., and Larsen, J.W., *Fuel*, **64**, 1668, (1985).
60. St. John, G.A., Butrill, Jr., S.E. and Anbar, M., *ACS Symposium Series*, **71**, p. 223 (1978).
61. Carangelo, R.M., Solomon, P.R. and Gerson, D.J., *Fuel*, **66**, 960, (1987).

62. Solomon, P.R. and Colket, M.B., *Fuel*, **57**, 748, (1978).
63. Brown, J.K., Dryden, I.G.C., Dunevein, D.H., Joy, W.K., and Pankhurst, K.S., *J. Inst. Fuels*, **31**, 259, (1958).
64. Orning, A.A. and Greifer, B., *Fuel*, **35**, 318, (1956).
65. Nelson, P.F., *Fuel*, **66**, 1264, (1987).
66. Calkins, W.H., Hagaman, E., and Zeldes, H., *Fuel*, **63**, 1113, (1984).
67. Calkins, W.H. and Tyler, R.J., *Fuel*, **63**, 1119, (1984).
68. Calkins, W.H., *Fuel*, **63**, 1125, (1985).
69. Calkins, W.H., Hovsepian, B.K., Drykacz, G.R., Bloomquist, C.A.A., and Ruscic, L., *Fuel*, **63**, 1226, (1984).
70. Solomon, P.R., Coal Structure, ACS Advances in Chemistry Series, **192**, 7, Washington, DC, (1981).
71. Freihaut, J.D., Proscia, W.M., and Seery, D.J., "Effect of Heat Transfer on Tar and Light Gases from Coal Pyrolysis", presented at the 194th National Meeting of the American Chemical Society, New Orleans, LA, (Aug. 31 - Sept. 4, 1987).
72. McMillen, D.F., Malhotra, R., Hum, G.P., and Chang, S.J., *Energy and Fuel*, **1**, 193, (1987).
73. Stein, S.E., New Approaches in Coal Chemistry, (B.D. Blaustein, B.C. Eockrath, and S. Friedman, Editors), ACS Symposium Series, **169**, 208, Am. Chem. Soc. Washington, DC, (1981).
74. Stein, S.E., "Multistep Bond Breaking and Making Processes of Relevance to Thermal Coal Chemistry", Annual Report for GRI Contract No. 5081-261-0556. Accession No. GRI-81/0147, (1983).
75. Stein, S.E., Robaugh, D.A., Alfieri, A.D., and Miller, R.E., "Bond Homolysis in High Temperature Fluids", *Journal of Amer. Chem. Society*, **104**, 6567, (1982).
76. Niksa, S., Paper No. 88-4 presented at the Western States Section/The Combustion Institute, Spring Meeting, Salt Lake City, Utah (March 1988).
77. Nelson, J.R., *Fuel*, **62**, 112, (1983).
78. Gerstein, Murphy, P.D., and Ryan, L.M., Coal Structure, (R.A. Meyers, Ed.) Chapter 4, Academic Press, New York, (1982).
79. Solum, M.A., Pugmire, R.J., Grant, D.M., and Wolfenden, W.R., "¹³C NMR Spectra of Coals in the Argonne Premium Coal Sample Bank", Submitted to *Energy and Fuel*, (1988).
80. Pitt, G.J., *Fuel*, **41**, 267, (1962).
81. Rennhack, "Zur Kinetik der Entgasung von Schmelzkoks," Brennstoff-Chemie, **45**, 300 (1964).
82. Hanbaba, P., Juntgen, H. and Peters, W., "Nicht-isotherme Reaktionskinetik der Kohlenpyrolyse, Teil II. Erweiterung der Theorie der Gasabspaltung und experimentelle Bestätigung an Steinkohlen," Brennstoff-Chemie, **49**, 358 (1968).
83. Van Heek, K.H., Juntgen, H. and Peters, W., "Kinetik nicht-isotherm ablaufender Reaktionen am Beispiel," Ber. Bunsenges, Phys. Chem., **71**, 113 (1967).
84. Gibbins-Matham, J. and Kandiyoti, R., ACS Fuel Div. Preprints, **32**, (4), 318, (1987).
85. Freihaut, J.D. and Seery, D.J., ACS Fuel Div. Preprints, **28**, (4) 265, (1983).
86. Serio, M.A., Peters, W.A., Sawada, K., and Howard, J.B., ACS Fuel Div. Fuel Preprints, **29**, (2), 65, (1984).
87. Serio, M.A., Solomon, P.R., and Carangelo, R.M., "Pyrolysis of the Argonne Premium Coals Under Slow Heating Conditions", ACS Div. of Fuel Chem., Toronto Meeting, (1988).

88. Solomon, P.R., Hamblen, D.G., Serio, M.A., Smoot, L.D., and Brewster, S., "Measurement and Modeling of Advanced Coal Conversion", First Annual Report for U.S. METC Contract No. DE-AC21-86MC23075, (1987).
89. Oh, M.S., "Softening Coal Pyrolysis", Sc.D. Thesis, Dept. Chem. Eng., MIT, Cambridge, MA, (1985).
90. Maiorella, B.L., "Behavior of Liquid Subbituminous Coal Tars Upon Heating, as it Relates to In-Situ Gasification", B.S. Thesis, Dept. Chem. Eng., MIT, Cambridge, MA, (1975).
91. Grey, J.A., Brady, A.J., Cunningham, J.R., Free, J.R., and Wilson, G.M., Ind. Eng. Chem. Proc. Des. Dev., 22, (1983).
92. Deshpande, G.V., Solomon, P.R., and Serio, M.A., "Crosslinking Reactions in Coal Pyrolysis", ACS Div. of Fuel Chem. Toronto Meeting, (1988).

SATISFACTION GUARANTEED

NTIS strives to provide quality products, reliable service, and fast delivery. Please contact us for a replacement within 30 days if the item you receive is defective or if we have made an error in filling your order.

▲ **E-mail: info@ntis.gov**

▲ **Phone: 1-888-584-8332 or (703)605-6050**

Reproduced by NTIS

National Technical Information Service
Springfield, VA 22161

This report was printed specifically for your order from nearly 3 million titles available in our collection.

For economy and efficiency, NTIS does not maintain stock of its vast collection of technical reports. Rather, most documents are custom reproduced for each order. Documents that are not in electronic format are reproduced from master archival copies and are the best possible reproductions available.

Occasionally, older master materials may reproduce portions of documents that are not fully legible. If you have questions concerning this document or any order you have placed with NTIS, please call our Customer Service Department at (703) 605-6050.

About NTIS

NTIS collects scientific, technical, engineering, and related business information – then organizes, maintains, and disseminates that information in a variety of formats – including electronic download, online access, CD-ROM, magnetic tape, diskette, multimedia, microfiche and paper.

The NTIS collection of nearly 3 million titles includes reports describing research conducted or sponsored by federal agencies and their contractors; statistical and business information; U.S. military publications; multimedia training products; computer software and electronic databases developed by federal agencies; and technical reports prepared by research organizations worldwide.

For more information about NTIS, visit our Web site at <http://www.ntis.gov>.

NTIS

**Ensuring Permanent, Easy Access to
U.S. Government Information Assets**



U.S. DEPARTMENT OF COMMERCE
Technology Administration
National Technical Information Service
Springfield, VA 22161 (703) 605-6000
